Post-stroke neural activities using electrocorticogram (ECoG) in a rat model of focal ischemia

ZHANG SHAOJIE

MASTER OF

PHILOSOPHY

THE HONG KONG POLYTECHNIC UNIVERSITY

2012

The Hong Kong Polytechnic University

Interdisciplinary Division of Biomedical Engineering

Post-stroke neural activities using electrocorticogram (ECoG) in a rat model of focal ischemia

ZHANG SHAOJIE

A thesis submitted in
partial fulfilment of the
requirements for the
degree of Master of
Philosophy

March 2012

CERTIFICATE OF ORIGINALITY

I hereby declare that this thesis is my own work and that, to the best of my knowledge and belief, it reproduces no material previously published or written, nor material that has been accepted for the award of any other degree or diploma, except where due acknowledgement has been made in the text.

_____

ZHANG Shaojie

March 2012

Abstract

An ischemic stroke lesion consists of ischemic core and penumbra. In the ischemic core, the neurons are damaged permanently because blood flow is reduced to a very low level. In the penumbra around the infarct core, the neurons are functionally impaired but structurally preserved. The structural and functional reorganization in penumbra facilitates recovery after stroke. However, delayed ischemia continues to develop in penumbra after the initial ischemia, and neuron survival in the penumbra is time-limited. Monitoring the ischemic penumbra is important for patient screening, treatment and prediction of recovery. MRI has made the visualization of the penumbra possible; however, MRI does not reliably detect damage in the first hours after stroke, and even may be misleading in some stroke cases. Consequently, the patients would miss the time window for effective therapeutic intervention. Moreover, MRI is costly and could only be performed for limited number of times per day. As an alternative, electrocorticogram (ECoG) provides a direct, convenient brain monitoring method by recording the electrical signals from surface of the cortex. However, the application of ECoG in experimental brain ischemia is not well studied. The objective of this study is to investigate the ECoG activities in a rat model of focal ischemia from the acute phase to the chronic phase.

In this study, focal cerebral ischemia was induced by intraluminal suture middle cerebral artery occlusion (MCAo), which produces a penumbra in sensorimotor cortex. Infarct maturation process and location of penumbra were revealed by 2,

3, 5-triphenyltetrazolium chloride (TTC) staining. Throughout the acute phase (after 3 and 6 hours), subacute phase (after 24, 48 and 72 hours) and chronic phase (after 96, 120, 144 and 168 hours), ECoG data were recorded from the bilateral sensorimotor cortex using stainless steel electrodes. The autoregressive model was applied to estimate the ECoG power spectrum density. The alpha-to-delta ratio (ADR), a quantitative ECoG parameter, was calculated from the ratio between the alpha power (8-13Hz) and the delta power (1-4Hz). Moreover, peak power variability was also calculated from ECoG recordings. The sensorimotor function and motor coordination were measured by De Ryck's test and beam walking test respectively.

The results from ECoG recordings showed suppression of ECoG amplitude in the penumbra during MCAo. ECoG power spectral analysis showed dominant delta activities in the acute phase and suppression of alpha/beta activities in the subacute phase, which possibly indicated striatum ischemia and delayed cortical ischemia at different stroke phases. Quantitative ECoG analysis showed the alpha/beta variability decreased during subacute phase and fully recovered in the chronic phase. ADRs were below 50% of the pre-stroke level at both acute and subacute phases, and the improvement in ADRs was highly correlated with sensorimotor function recovery (Pearson's correlation, $r = 0.9895$, $p<0.05$). In addition, TTC stained brain slices confirmed that striatum infarct completed within 24 hours and the cortical infarct expanded until 72 hours.

Altogether, this study demonstrated that ECoG provided information on the

stroke pathophysiology in a rat model of focal ischemia from acute phase to chronic phase. Post-stroke functional recovery was closely related to the restoration of neural activity in the penumbra. Quantitative ECoG parameters, such as ADR and peak power variability, have the potential to be used in stroke diagnosis and prognosis.

PUBLICATIONS & AWARDS ARISING FROM THE THESIS

Publications

1. **Shaojie Zhang**, Kaiyu Tong, Zheng Ke, Changes of temporal profile of Electrocorticogram in ischemic penumbra after focal ischemia in rats, *poster presentation in 41th annual meeting of society for neuroscience, Washington DC, USA, Nov 2011.*

2. **Shaojie Zhang**, Zheng Ke, Le Li and Kaiyu Tong, Electrocorticogram reveals penumbral delayed ischemic damage and sensorimotor recovery after stroke, under submission

3. Zheng Ke, Michael Ying, Le Li, **Shaojie Zhang**, Kaiyu Tong. Evaluation of transcranial doppler flow velocity changes in intracerebral hemorrhage rats using ultrasonography. Journal of Neuroscience Methods 210 (2012): 272-280.

Awards

4. **Shaojie Zhang**, 1st runner-up of Hong Kong Medical and Healthcare Device Industries Association Student Research Award (2011)

5. **Shaojie Zhang**, Final list of 3rd IEEE EMBS Hong Kong Chapter Student Paper Competition (2011)

ACKNOWLEDGEMENTS

I would like to express my sincere thanks to my chief supervisor, Dr. Kai-yu Tong, Raymond, for his professional guidance, full support and encouragement throughout my postgraduate study.

Besides, I would like to express my appreciation to my colleagues Dr. Le Li, Dr. Xiaoling Hu, Dr. Zheng Ke, Wei Rong, Teris Tam and other colleagues from Department of Health Technology and Informatics. Special thanks would be given to Dr. Le Li and Dr. Zheng Ke, for their teaching and assistance in experimental techniques and useful advice during my postgraduate study. In the meanwhile, I would also gratefully acknowledge the husbandry supports from Centralized Animal Facilities (CAF) of the Hong Kong Polytechnic University.

Finally I would sincerely thank my family and my friends in PolyU for their great support during my postgraduate study.

This study is funded by the Hong Kong Research Grants (PolyU 5292/08E).

Shaojie Zhang

March 2012

TABLE OF CONTENTS **Page**

List of Abbreviations

ACA	Anterior cerebral artery
ADR	Alpha to delta ratio
AIS	Acute ischemic stroke
AR	Autoregressive
CBF	Cerebral blood flow
CCA	Common carotid artery
ECA	External carotid artery
ECoG	Electrocorticography
EEG	Electroencephalography
fMRI	functional magnetic resonance imaging
ICA	Internal carotid artery
MRI	Magnetic resonance imaging
MCA	Middle cerebral artery
MCAo	Middle cerebral artery occlusion
PCA	Posterior cerebral artery
PDA	Polymorphic delta activity
PID	Peri-infarct depolarization
PSD	Power spectrum density
qEEG	quantitative Electroencephalography
TTC	2, 3, 5-triphenyltetrazolium chloride
TUNEL	Terminal deoxynucleotidyl transferase dUTP nick end labeling

List of Figures

List of Tables

CHAPTER 1 INTRODUCTION

1.1 Definition of stroke

Stroke, or cardiovascular accident, is a life-threatening condition marked by a sudden disruption in the cerebral blood supply, which causes neurons to die within minutes due to the deprivation of oxygen and glucose (Doyle et al., 2008). Stroke is the third leading cause of death, following heart disease and cancer. According to the American Stroke Association statistics, 795,000 Americans experience a new or recurrent stroke each year, which means a stroke occurs every 40 seconds. Nearly 30% of patients die within one year after a stroke, and the percentage increases among older person. About 40% of stroke-related deaths occur in males, and 60% in females (Roger et al., 2011).

In addition, stroke is a major cause of disability. Depending on the brain area that is damaged, persons who have a stroke subject may have certain functions impaired, such as speech, movement, behavior and learning. The loss of function may be temporary or permanent, mild or severe. The following characteristics are very common among stroke survivors over 65 years of age (Roger et al., 2011):

- 50% had some hemiparesis
- 30% were unable to walk without some assistance
- 26% were dependent in activities of daily living
- 19% had aphasia
- 35% had depressive symptoms
- 26% were institutionalized in a nursing home.

The economic burden directly and indirectly caused by stroke is immense. Americans paid about $73.7 billion for stroke-related medical costs and disability in 2011 (Roger et al., 2011).

1.2 Stroke classification

Stroke is classified into three subtypes: ischemic stroke, transient ischemic attack (TIA) and hemorrhagic stroke. Ischemic stroke is caused by thrombosis or embolism. A thrombosis is a blood clot that develops at the clogged blood vessel and an embolism is a blood clot that travels to the clogged blood vessel from other parts in the circulatory system (Figure 1.1a). TIA is caused by a temporary clot that tends to resolve itself quickly, usually within 10-20 minutes. TIA does not require a particular intervention; however, it is a strong indicator of an ischemic stroke and should be evaluated in the same way as a stroke to prevent a more serious stroke from occurring (Roger et al., 2011) (Figure 1.1b). Hemorrhagic stroke is caused by vessel bleeding within the brain (intracerebral hemorrhage) or between the inner and outer layers of the tissue covering the brain (subarachnoid hemorrhage) (Figure 1.1c). If a diagnosis between ischemic stroke and hemorrhagic stroke can be made in the emergency stage, the correct treatment can be initiated more quickly.

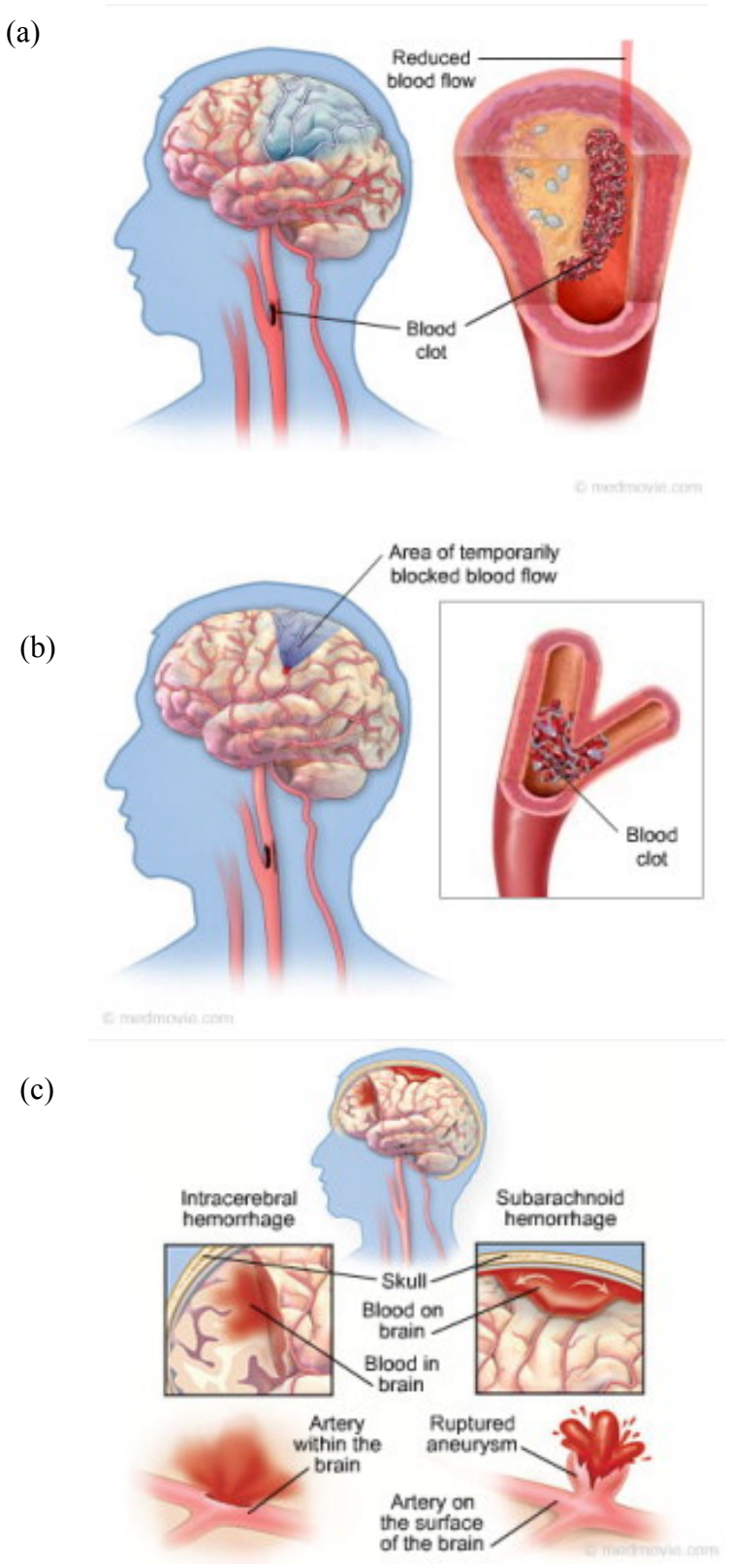

Figure 1.1 Stroke classification. (a) Ischemic stroke. (b) Transient ischemic attack. (c) Hemorrhagic stroke. Aneurysm and vessel malformations are likely to develop a hemorrhagic stroke (American heart and stroke association).

1.3 Stroke diagnosis

Stroke diagnosis is important because the treatment depends on the type, the source (related to risk factors), and the location of the stroke in the brain. Generally, neuroimaging, cerebral blood flow (CBF) test and electrical activity test are common tools in stroke diagnosis.

Magnetic resonance imaging (MRI) and computer tomography (CT) scans show the location and severity of a stroke. The MRI scan is sharper and more detailed than a CT scan so it can be used to diagnose small, deep injuries.

Ultrasound can measure blood flow in carotid arteries and vertebral arteries. Also, cerebral angiography uses an X-ray scan to visualize the size and location of blockages in the blood vessel. This test is valuable in diagnosing aneurysms and malformed blood vessels and providing valuable information before surgery.

Electroencephalogram (EEG) test uses electrodes placed on a patient's scalp to pick up electrical signals. An evoked response test measures how the brain' responses to sensory stimulations.

1.4 Stroke treatment

The effective treatment for stroke is limited. The most promising stroke treatment is tissue plasminogen activator (t-PA) induced thrombolysis (Carmichael, 2005). Currently, t-PA is the only therapy for acute ischemic stroke (AIS) approved by the US Food and Drug Administration. In Hong Kong, the Stroke Thrombolysis Team at Prince of Wales Hospital and Queen Mary Hospital provides t-PA treatment for

patients with AIS within 24 hours. Early administration of t-PA benefited a carefully selected patient group with acute stroke. Despite proven efficacy, utilization rates of t-PA remain low (Leung et al., 2011).

In addition, many neuroprotective drugs are proved to be effective in animals, but their failure in clinical trials may be due to unpredictable psychological and psychiatric adverse effects.

1.5 Objectives

Stroke does not affect the ischemic territory homogeneously. Permanent neuron death develops in the infarct core within minutes after ischemia; whereas delayed ischemia could continue to develop after initial ischemia. It is necessary to have comprehensive understanding of the brain activity and tissue status in penumbra over time. The objectives of this study are:

1. To indentify the ischemic penumbra in a rat model of focal cerebral ischemia and set up an ECoG recording system for neural activities in penumbra.
2. To characterize ECoG patterns at different post-stroke phases after focal cerebral ischemia, with respect to changes in delta (1-4Hz), theta (4-7Hz), alpha (8-12Hz) and beta (13-30Hz) bands.
3. To evaluate the relationship between quantitative ECoG parameters and functional recovery.

1.6 Outline of the thesis

Chapter 2 reviews the current understanding of stroke pathophysiology, the stroke rat models, and stroke outcome evaluation by neuroimaging, neurophysiology and histological methods.

Chapter 3 describes the methodology to illustrate the experiment setup including intraluminal suture middle cerebral artery occlusion, ECoG recording and analysis. The motor function assessments and histological method are also described.

Chapter 4 shows the results of histology, functional assessment and ECoG characteristics after stroke.

Chapter 5 discusses the possible relationship between post stroke neural activities and functional recovery. In addition, this chapter points out the limitations in the study and makes suggestions for future work.

Chapter 6 summarizes the major findings of this study and the potential implications of EEG in stroke diagnosis.

CHAPTER 2 LITERATURE REVIEW

2.1 Stroke pathophysiology

2.1.1 Cerebral circulation

Since the cerebral vascular system has an important bearing upon stroke etiology, it is important to introduce circle of Willis in the beginning of this chapter.

The circle of Willis is formed when the internal carotid artery (ICA) enters the cranial cavity and divides into the anterior cerebral artery (ACA) and middle cerebral artery (MCA). The ACAs are united by an anterior communicating artery (ACom). These connections form the anterior part of the circle of Willis (Figure 2.1). In the posterior part, the basilar artery, formed by the bilateral vertebral arteries, branches into a posterior cerebral artery (PCA), forming the posterior circulation (Figure 2.1). The PCA joins the circle of Willis via the posterior communicating artery (PCom).

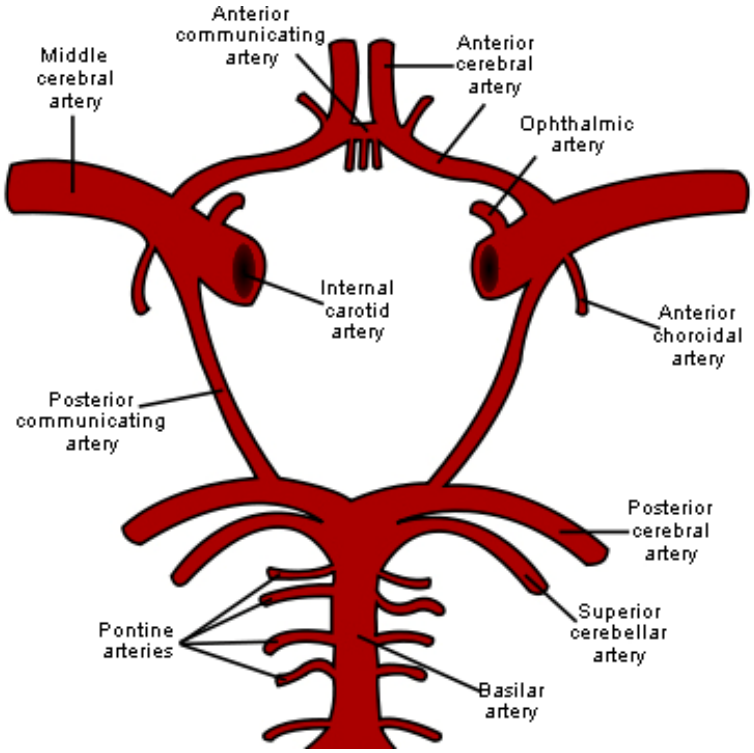

Figure 2.1 Circle of Willis

MCA proximal branches, namely lenticulostriate arteries, supply the internal capsule, part of the caudate putamen and globus pallidus. MCA distal branches supply most of the temporal lobe, frontal lobe, and parietal lobe (Figure 2.2). Most of the ischemic stroke results from MCA occlusion (Durukan and Tatlisumak, 2007). Right MCA occlusion causes contralesional hemiplegia and ipsilesional head/eye deviation, and left MCA occlusion causes global aphasia.

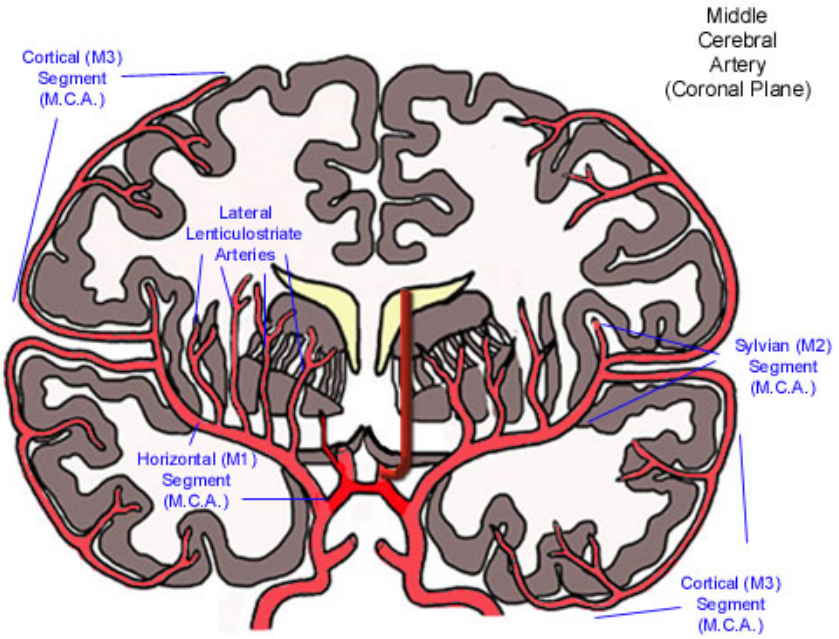

Figure 2.2 M1, M2 and M3 branches of MCA. The lenticulostriate arteries from M1 segment of MCA, and they are end arteries.

2.1.2 Core and penumbra

An stroke lesion consists of ischemic core and the penumbra (Hofmeijer and van Putten, 2012) (Figure 2.3). In the ischemic core, the complete loss of blood perfusion (4.8-8.4 mL/100g/min) leads to energy failure and causes permanent neural death, a situation that may be delayed by neuroprotective drugs but hardly prevented. In the penumbra, the brain tissue remains partially perfused (14-35mL/100g/min), but the

blood perfusion in penumbra is not sufficient for axonal and synaptic activity (Heiss, 2011). In a macroscopic perspective, observations of permanent neurological disturbances without relevant lesions on diffusion magnetic resonance imaging (DWI) in the acute, subacute and chronic phase suggest the neurons in the penumbra are intact and viable, but functionally impaired (Hofmeijer and van Putten, 2012). In a microscopic perspective, structural degeneration was only found in the post-synaptic dendrite spines without neuronal or axonal damage after 10% of blood flow reduction, and this structural change is reversible if reperfusion occurs within 20-60 min (Zhang et al., 2005). Failure of synaptic transmission has been proposed to account for electric silence in the penumbra (Hofmeijer and van Putten, 2012).

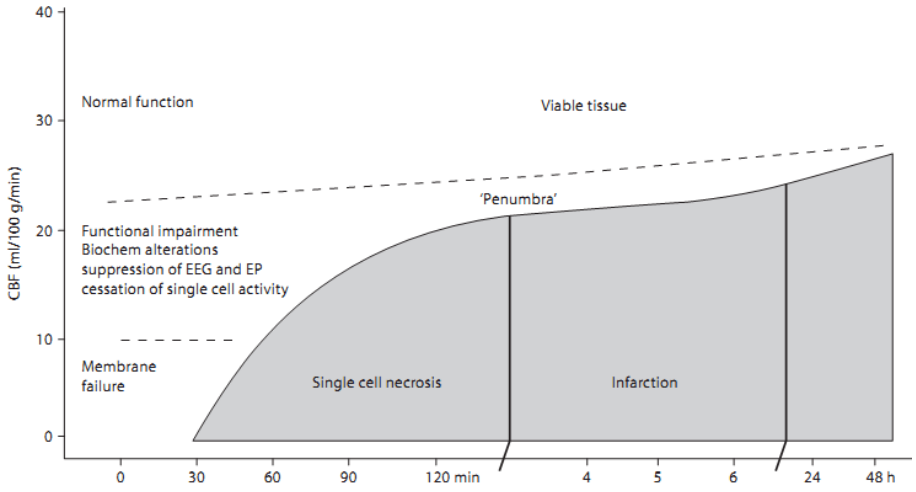

Figure 2.3 Blood flow threshold concept of ischemia. The declining flow rate is associated with penumbra and infarct core. The solid line separates core from penumbra. The dashed line distinguishes viable from functionally impaired tissue.

Brain injury following focal cerebral ischemia develops from a series of complex pathological events in a delayed style. Factors including energy failure, excitotoxicity, peri-infarct depolarizations (PIDs), inflammation and apoptosis contribute to delayed

secondary ischemia (Dirnagl et al., 1999) (Figure 2.4). Delayed ischemia could last hours, days and even weeks. The spatiotemporal profile pathophysiological process can be characterized in the animal models; however to identify the heterogeneous pathophysiological process noninvasively in stroke patients is very difficult. The penumbra might exist for a shorter time period in stroke patients (Dirnagl et al., 1999). Therefore, neuron survival in penumbra is a time limited process. The capacity of neurological recovery is closely related to ultimate survival of penumbra. Therapeutic interventions that prevent infarction of penumbra may reduce neurological impairment (Furlan et al., 1996).

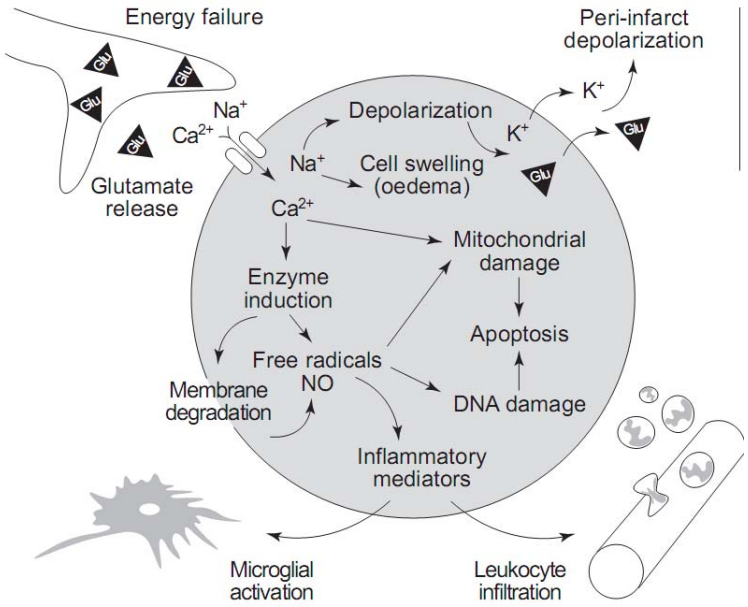

Figure 2.4 Pathophysiological mechanisms of focal cerebral ischemia (Dirnagl et al., 1999).

2.1.3 Energy failure and excitotoxity

The brain is the most metabolically active organ in the body. While taking only 2% of the body mass, it consumes 20% of glucose and oxygen. Impairment of cerebral blood flow restricts the delivery of oxygen and glucose, and impairs the energy

required to maintain ionic balance. With energy depletion, membrane potential is lost and neurons depolarize. Excitatory amino acids, especially glutamate from presynaptic neuron, are released into the extracellular space in large amount (Durukan and Tatlisumak, 2007). The activation of glutamate receptors will induce an abnormally high elevation of intracellular Ca^{+}, Na^{+} and Cl^{-} concentration leading to subsequent cell damage like edema and necrosis (Durukan and Tatlisumak, 2007). Although blocking glutamate receptors protects against excitotoxicity, it can also have serious unwanted effects, such as psychotic symptom, respiratory depression or cardiovascular dysregulation.

2.1.4 Peri-infarct depolarizations (PIDs)

In the ischemic core, neurons can undergo an anoxic depolarization and never repolarize. In the penumbra, neurons can repolarize and depolarize again in response to increasing extracellular glutamate at the expense of further energy consumption. Clinical evidence shows PIDs exist in human subject when suffered from conditions like focal ischemia and bran trauma (Fabricius et al., 2006). The influence of PIDs on hemoglobin oxygenation can be detected with near-infrared optical spectroscopy as well as blood oxygen level-dependent (BOLD) MRI (Dirnagl et al., 1999). PID is a large negative DC potential shift of 10-20 mV, between 40 seconds and 5 minutes in duration, occurring in frontal and parietal lobe (Hartings et al., 2006). PID moves from ischemic core to penumbra at a slow speed about 3mm/min (Mies G et al., 1993). The frequency of PID recurrence matches the progression of infarct growth,

but few PIDs would occur beyond 24h in stroke rat model (Hartings, Rolli, et al., 2003). Drugs containing NMDA and AMPA receptor antagonists could block PIDs, thus reduce infarct volume (Lu et al., 2005).

2.1.5 Inflammation

Ischemic injury also triggers inflammatory cascades in the brain parenchyma that may further exacerbate tissue damage. Neutrophils arrive at the ischemic tissue within hours after reperfusion (Emerich et al., 2002). The pathogenic role of neutrophils and other leukocytes in cerebral ischemia is still under debate. Neutrophils migration may worsen the degree of ischemia by occluding micro-vessels (Emerich et al., 2002).

Besides, production of toxic mediators by inflammatory cells and injured neurons can amplify brain damage. Infiltrating neutrophils produce toxic amount of nitric oxide. Ischemic neurons express COX2, an enzyme that mediates ischemic injury by producing superoxide, and tumor necrosis factor α, a cytokine that can exacerbate ischemic injury (Durukan and Tatlisumak, 2007). Treatments that can down-regulate the neutrophilic infiltration and inhibit toxic mediators could be viable strategies for later phases of stroke (Dirnagl et al., 1999).

2.1.6 Necrosis and apoptosis

Neurons that are compromised by excessive glutamate receptor activation, calcium overload, oxygen radicals, mitochondrial damage or DNA damage can die either by necrosis or by apoptosis. This decision depends on the nature and intensity of the

stimulus, cell type, and the stage in life cycle (Dirnagl et al., 1999). Necrosis is the predominant cell death type in the ischemic core following acute permanent vascular occlusion, and it is resistant to neuroprotective drugs administered. Apoptosis plays an important role in the development of delayed ischemia in the penumbra. The time course of apoptosis is consistent with that of infarct development, especially in dorsolateral cortex (Xu et al., 2006). Apoptosis contributes to cell replacement, tissue remodeling and removal of damage cells. The initial ischemic stimulus induces expression of genes which eventually lead to apoptotic cell death (Dirnagl et al., 1999). In rat MCAo model, cortical infarction contains a greater degree of apoptotic cell death than in striatum infarction (Carmichael, 2005).

2.2 Modeling focal cerebral ischemia

Various rodent stroke models have been established in which the blood flow is acutely or slowly, completely or incompletely, focally or globally, permanently or transiently reduced. Rodent stroke models provide the experimental basis for the *in vivo* study of the mechanisms of brain injury and repair, and for the testing of neuroprotective drugs (Carmichael, 2005).

2.2.1 Thromboembolic model

Thromboembolic stroke model mimics human stroke most closely since most of the human strokes are caused by thromboembolism. Advantages of this model are their potential to test thrombolytic agents, to evaluate the ischemic lesion which undergoes thrombolysis and to test the combined therapies of thrombolytic drugs and

neuroprotective drugs (Durukan and Tatlisumak, 2007).

Early thromboembolic ischemia is induced by injection of autologous thrombi into extracranial arteries to reach the distal arteries. Infarcts induced by human blood clot or a suspension of homologous small clot are variable and early spontaneous recanalization occurs (Hossmann, 2008). Therefore efforts have been made to induce consistent CBF decline and reproducible lesions. Busch et al. sequentially injected fibrin-rich autologous clots and consistently reduced CBF in the MCA, without any spontaneous recanalization 3h after embolization (Busch et al., 1997).

2.2.2 Intraluminal suture model

The intraluminal suture method is the most frequently used experimental stroke model. This model mimics the condition of large artery occlusion, and is technically easy to perform both permanent and transient focal cerebral ischemia in a controlled manner. Since Koizumi's first introduce the intraluminal suture MCAo in rats (Koizumi et al., 1986) (Figure 2.5a), several modifications have been made (Longa et al., 1989; Durukan and Tatlisumak, 2007) (Figure 2.5b). This model requires insertion of a suture into the ICA and advancing until it blocks blood flow to MCA at its origin. Therefore, suture MCAo affects M1, M2 and M3 branches of MCA (Figure 2.2). The suture can be left in ICA for a variable duration of time and then removed to produce reperfusion. The most common durations of MCA occlusion are 60min, 90min, and 120 min as well as permanent occlusion (Carmichael, 2005).

Lesion reproducibility and size are affected by suture diameter (3.0 or 4.0 filament),

coating of the suture (with silicone or poly-l-lysine), and insertion depth of the thread. Size of the suture and the depth of suture insertion correlates well with the infarct volume (He et al., 1999; Abraham et al., 2002). Silicone coated suture causes larger and more consistent infarcts with good reproducibility and reliability than uncoated suture (Shimamura et al., 2006).

Table 2.1 Anatomic structures involved in intraluminal method (S: striatum, C: cortex)

Ischemic core (S)	Caudate Putaman; Globus pallidus
Ischemic core (C)	Parietal cortex, agranular insular cortex
Inner boundary zone (S)	Medial-dorsal caudate putamen; medial globus pallidus
Inner boundary zone (C)	Forelimb area of cortex
Outer boundary zone (S)	Medial-dorsal caudate putamen; medial globus pallidus
Outer boundary zone (C)	Hindlimb area of cortex

This model produces infarction in the both frontoparietal cortex (somatosensory cortex and sensorimotor cortex) and lateral caudal putamen (Table 2.1). Since the anatomy and physiology of sensorimotor cortex are well studied, studying this model allows the investigation of stroke recovery mechanism in the sensorimotor circuits (Carmichael, 2005).

Disadvantages of this method include: vessel rupture, subsequent subarachnoid hemorrhage, hyperthermia and inadequate occlusion. Silicone coated suture and laser Doppler guided placement of the suture could reduce the incidence of subarachnoid hemorrhage (Elsaesser-Schmid et al., 1998). Spontaneous hyperthermia is associated with hypothalamic injury and occurs in most animals if the occlusion is longer than 2h (Dogan et al., 1999). Continuous efforts are being made to optimize suture design and methodology of suture technique (Ma et al., 2006).

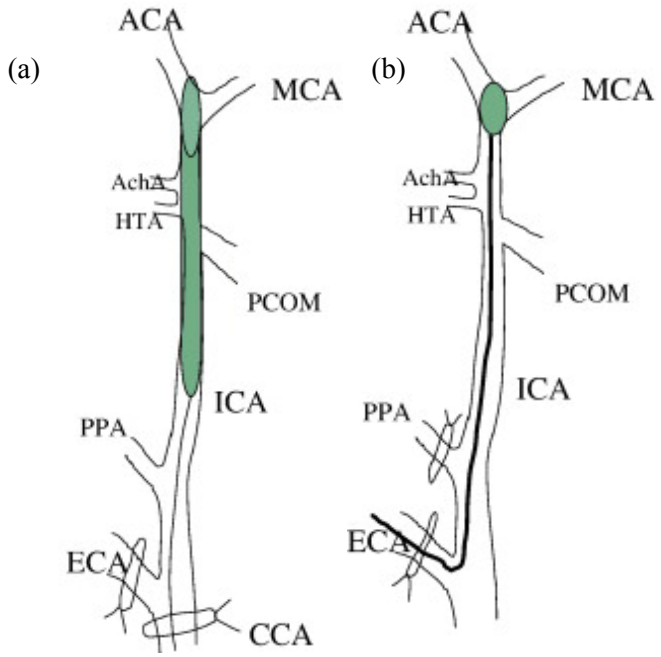

Figure 2.5 Intraluminal suture middle cerebral artery occlusion. (a) Koizumi's method, insertion of the silicone-coated suture into common carotid artery (CCA), blocking MCA, anterior choroidal artery (AchA), and hypothalamic artery (HTA). (b) Longa's method, insertion of the uncoated suture from external carotid artery to the bifurcation of ACA and MCA.

2.2.3 Photothrombosis model

Photothrombosis produces a cortical infarct by systemic injection of a photoactive dye in combination with irradiation by a light beam at a specific wavelength (Watson et al., 1985). Generation of singlet oxygen leads to focal endothelial damage, platelet aggregation in both surface and penetrating vessels within the irradiated area (Sigler et al., 2009) (Figure 2.6). This model is end artery occlusion in nature and is resistant to therapies based on collateral blood supply (Durukan and Tatlisumak, 2007). Photothrombosis could induce ischemic lesion in any desired cortical area, but it cannot produce lesion in the subcortical region. Besides, this model lacks of penumbra because vasogenic edema and BBB breakdown occur within minutes in the lesion, thus it is undesirable for preclinical drug studies targeting at penumbra.

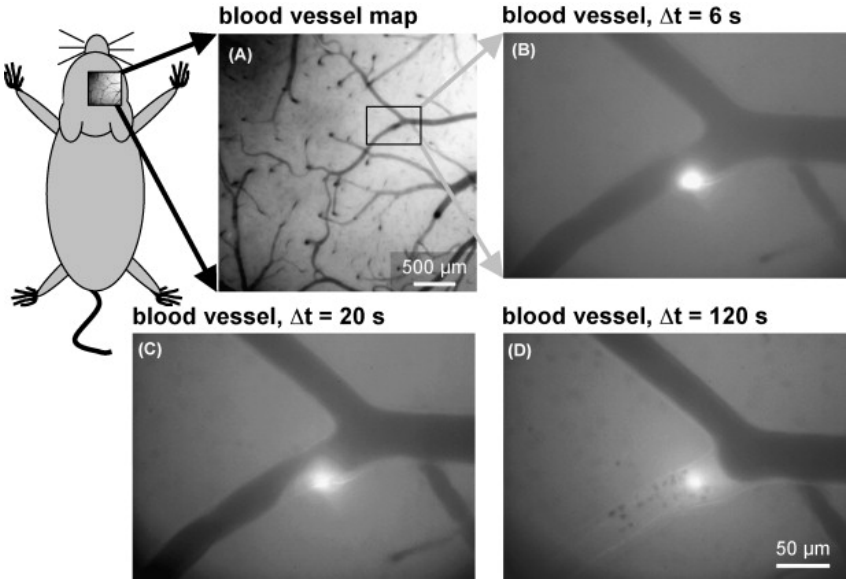

Figure 2.6 Photothrombosis model. (a) Blood vessel targeting for photoactivation indicated by arrows. (b) Photoactivation spot in the vessel visualized by fluorescence activation with laser. Blood flow in this vessel is partially blocked at 20s (c) and completely blocked within 120s (d).

2.2.4 Endothelin-1 induced stroke

Endothelin-1 (ET-1) is a vasoconstrictor that can be applied directly on the exposed MCA (Macrae et al., 1993), adjacent to the MCA by stereotaxic intracerebral injection (Sharkey et al., 1993) or onto the cortical surface. Application of ET-1 in the proximal MCA provides significant decrease of CBF (70-93%) in the distal MCA, which results in ischemic lesion pattern similar to that induced by suture method (Figure 2.7). Cortical application of ET-1 provides sufficient reduction in CBF and induce a semicircular infarct involving all layers of the neocortex (Fuxe et al., 1997). Less invasiveness and ability to induce ischemia in any desired region of the brain are the major advantages of this model, but dose dependent action of ET-1 reduces the control on ischemia duration and intensity. Moreover, ET-1 application may induce axonal sprouting that may interfere with the interpretation of neural repair (Carmichael, 2005).

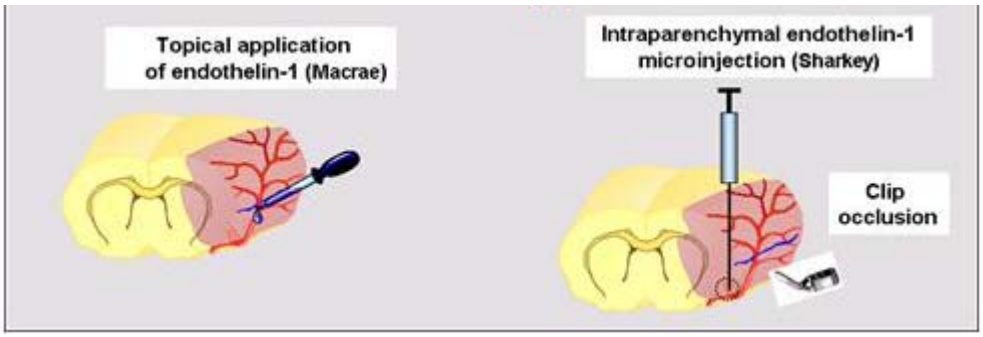

Figure 2.7 Methods of ET-1 injection. (a) Topical application through craniotomy (b) Intracerebral injection

2.3 Neuroimaging

Neuroimaging is a powerful tool to assess the cerebral tissue status after stroke noninvasively. The ultimate goal of neuroimaging is to define the brain regions of infarction and perfusion deficit, and to identify any ischemic tissue that can be salvaged by medical treatment (Hossmann, 2008). MRI parameters include apparent diffusion coefficient (ADC) in diffusion weighted imaging (Figure 2.8), BOLD signal, and the transverse relaxation time T2 to visualize edema formation. However, none of these parameters exhibits a sharp threshold relationship to declining CBF and does not provide a clear differentiation between the ischemic core and the penumbra. Besides, MRI is not sensitive enough to evaluate acute stroke. T2-weighted imaging can detect acute stroke by 6-12h, however, most of the neuroprotective agents are not effective beyond 3h time window. Normal findings on MRI after mild transient ischemia may not indicate normal tissue status (Sicard et al., 2006).

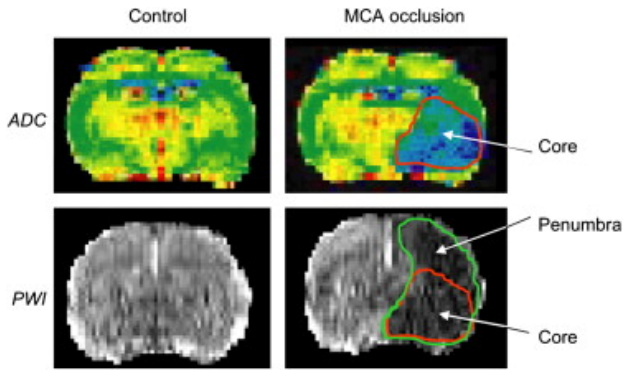

Figure 2.8 Penumbra is the mismatch between the ADC maps (with increased signal intensity) and perfusion weighted imaging (Hossmann, 2008)

2.4 Functional evaluation

In line with the clinical relevance, a number of behavior tests have been established, mainly focusing on skilled limb use, sensorimotor integration, motor coordination and balance (Brooks and Dunnett, 2009).

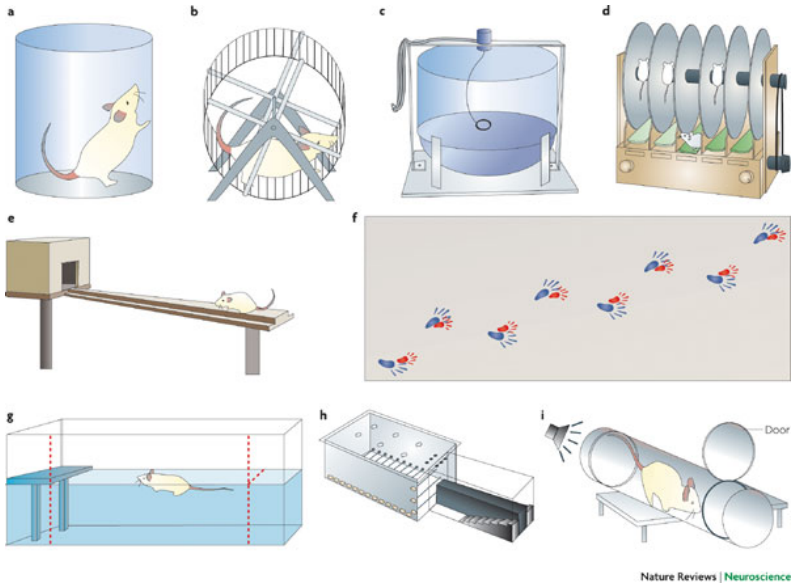

Figure 2.9 Functional tests. (a) Cylinder test (b) Running wheel test (c) Rotometer test (d) Rotarod test (e) Raised beam walking (f) Footprint analysis (g) Swimming test (h) Staircase reaching test (i) Acoustic startle chamber (Brooks and Dunnett, 2009)

2.4.1 Locomotor activity test

Wheel running measures voluntary locomotor activity. The total number of wheel

rotations, the speed of running, the time to initiate running and the number of breaks from running can all be used as measurements of activity (Harri et al., 1999).

Rotometer test measures the extent of lateralized lesions by observing the animals' rotational bias, typically after administration of a psychomotor stimulant drug (Ungerstedt and Arbuthnott, 1970).

2.4.2 Limb use

Cylinder test detects forelimb impairments in rodents with unilateral lesion, and has proved to be a simple and efficient test of unilateral deficits in voluntary forelimb use. Forelimb function is assessed by the number of instances the rat uses its paw to touch the cylinder (Schallert et al., 2000).

Reaching test investigates the forelimb use and motor dysfunctions after brain damage. It requires the rodent to reach through the bars of a wire mesh cage to retrieve food pellets, and the reaching success is rated (Whishaw et al., 1986).

Staircase reaching test is sensitive to ischemic lesions (Bouët et al., 2007). The rodents can use only the forelimb on the same side as the staircase to retrieve pellets. This test provides a direct and simple measurement of lateralized impairments and forepaw dexterity (Brooks and Dunnett, 2009).

2.4.3 Motor coordination and balance

Rotarod test was designed for making automated measurements of neurological deficits in rodents. In this test, rats are placed on the beam that can rotate at a fixed or an accelerating speed and their latency to fall provides a measurement of their motor

coordination (Dunham and Miya, 1957).

Beam walking evaluates the rodent's ability to traverse the beam, which is considered as an indication of balance. Paw slips and traverse time are used as the measurements (Jolkkonen et al., 2000).

Gait analysis examines the motor coordination and synchrony during walking. The forelimbs and hindlimbs are painted with dyes of different colors and the rodent is encouraged to walk in a straight line over absorbent paper. Stride length, base width and overlap between forelimbs and hindlimbs are analyzed for gait pattern (Clarke and Still, 2001).

2.5 Histological methods to study ischemia

Histological staining, immunohistochemistry, and enzyme histochemistry analyze the ischemic neural damage (Sommer, 2010). While infarct volume calculation is feasible with all the above methods, plans to perform further analysis of gene expression, protein expression, lactate, ATP, and receptor binding densities may require specific tissue preprocessing techniques. Cryostat or PFA-fixed tissue would allow reaction with antibodies for immunohistochemistry and paraffin-embedded tissue provides the best results in neuron morphology.

2.5.1 Hematoxylin and eosin staining

Hematoxylin and eosin (H&E) staining is routinely used in diagnostic pathology, and it is a valuable tool for detecting ischemic brain lesions (Figure 2.10). This staining

allows for the detection of selective neuronal death in penumbra. While normal brain tissue stains eosinophilic-red, the infarct region appears pale. The distinction between infarct and adjacent tissue is possible after 24h (Sommer, 2010).

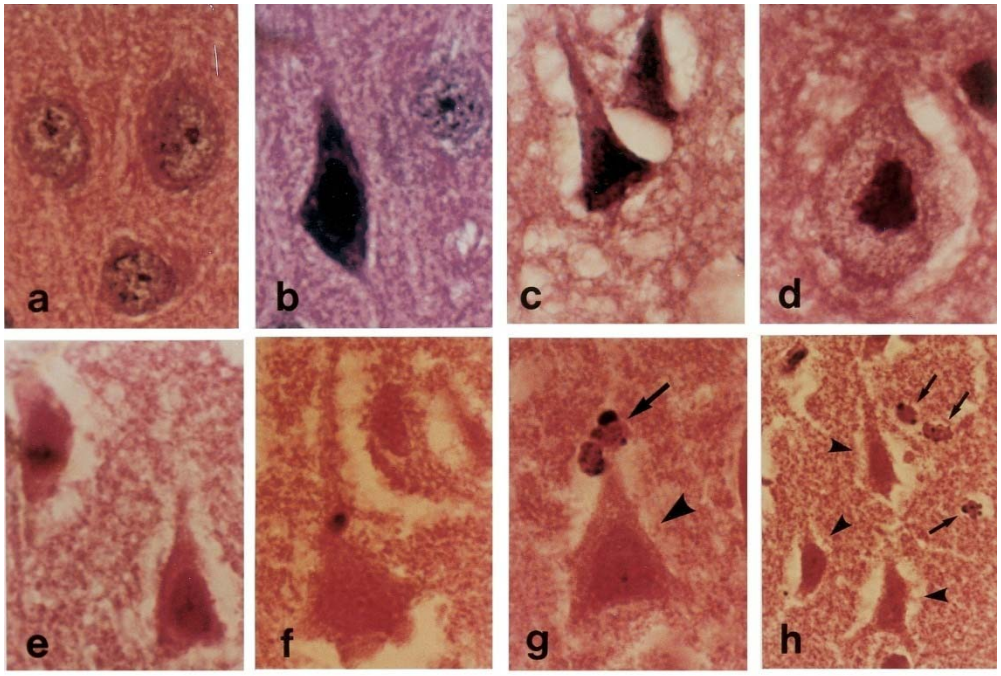

Figure 2.10 Structural features of intact, injured, necrotic and apoptotic neurons on H&E staining after MCAo. (a) intact neuron in the contralesional cortex (b) non-scalloped shrunken dark neurons in the contralesional cortex (c) scalloped shrunken dark neurons (d) swollen neurons (e) red neurons (f) ghost neurons in the core (d) swollen neurons in the core (g-h) necrotic (arrow heads) and apoptotic (arrows) cells (Li et al., 1998).

2.5.2 Microtubule-associated protein (MAP2) staining

MAP2 is a well established marker protein for the early detection of brain ischemia. Reduced MAP2 staining has been reported as early as 1h following the ischemia onset (Sommer, 2010). A good correlation between MAP2 staining and T2-weighted MRI has been reported (Kloss et al., 2002). The limitation with MAP2 staining is MAP2 protein mainly existing in dendrites rather than axon, and detecting white matter damage is problematic (Sommer, 2010).

2.5.3 2, 3, 5-triphenyltetrazolium chloride (TTC) staining

The use of TTC staining for infarct quantification in stroke rat models dates back to the 1980s (Bederson et al., 1986). The red stain intensity correlates with the number and functional activity of mitochondria with complete lack of TTC staining indicating infarct core (Bederson et al., 1986). This method is easy to apply and the results are immediately available, revealing a high contrast between normal and infarct tissue and allowing for automated image analysis (Goldlust et al., 1996). Furthermore, TTC stained brain slices can theoretically be used for additional histological and immunohistochemical staining, although the result is not ideal (Popp et al., 2009). However, TTC only labels mitochondria, and tissues with a low density of mitochondria (i.e., white matter) are lack of red stain, which makes demarcation of the infarct problematic (Figure 2.11b). The second limitation is the narrow time window. Although TTC staining has been reported to delineate infarcts as early as 3h in severe ischemia, reliable detection of infarcts after mild ischemia requires about 24 hours (Popp et al., 2009).

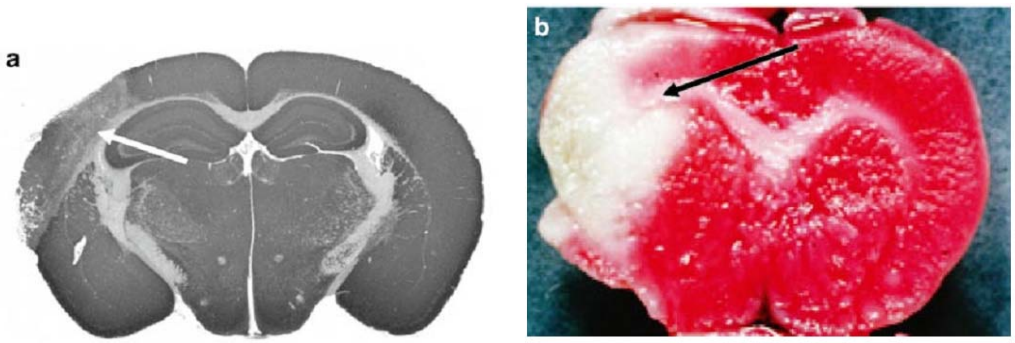

Figure 2.11 MAP2 and TTC staining. The border between infarct and normal tissue is clear in the cortex after MAP2 staining (a) and TTC staining (b) However, involvement of the white matter can hardly be distinguished from the white colored infarct (arrows) (Sommer, 2010).

2.5.4 Staining for selective neuron death

Selective neuron death in penumbra has to be distinguished from necrosis (Section 2.1.6). Generally, the morphology of selectively injured neurons can be indentified one week after ischemia using terminal deoxynucleotidyl transferase mediated dUTP-biotin nick end-labeling (TUNEL, Figure 2.12) or fluoro-Jade B, an anionic fluorescent marker of cell death (Hermann et al., 2001; Hossmann, 2008; Liu et al., 2009).

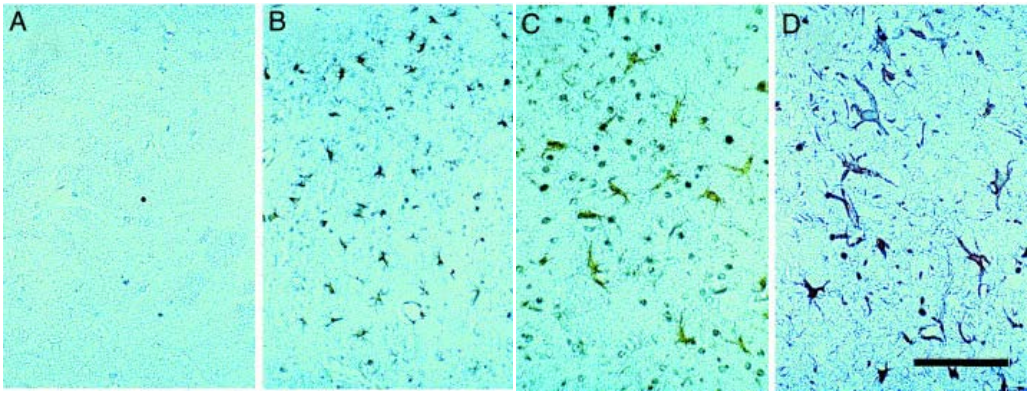

Figure 2.12 Evolution of apoptosis after focal cerebral ischemia. Dark round neurons are TUNEL positive cells after reperfusion following MCAo. Tissue sections were obtained at 24h (a), 48h (b), 72h (c) and 7d (d). Numbers of TUNEL-positive cells are low at 24h, increased at 72h and decreased at 7 days (Dirnagl et al., 1999).

2.6 Neurophysiology

2.6.1 Electrical signals from the brain

Based on the location of signal source, electrical activities from brain include EEG, electrocorticography (ECoG), filed potentials and single neuron activity (Figure 2.13a). EEG is the recording of the electrical activity from the scalp. The spatial resolution of EEG is reduced by the skull thus EEG electrodes cannot detect charges outside 6cm^2 of the cortical surface, and the effective recording depth is several

millimeters (Thakor and Tong, 2004). EEG rhythms are the summation of excitatory and inhibitory postsynaptic potentials produced in the the cerebral cortex.

Different from EEG, ECoG is the recording of electrical brain activities directly from cortical surface and craniotomy is required. ECoG has a superior spatial resolution and wider spectral range (Figure 2.13b). ECoG contains delta, theta, alpha, beta rhythms as well as higher frequency gamma rhythms (30-200Hz), which are not visible in EEG recordings (Daly and Wolpaw, 2008). ECoG is free of contamination from non-brain signals. It can record the field potential within a few mm² of cortical surface, which allows activity of a population of neurons within a volume of tissue..

(a)

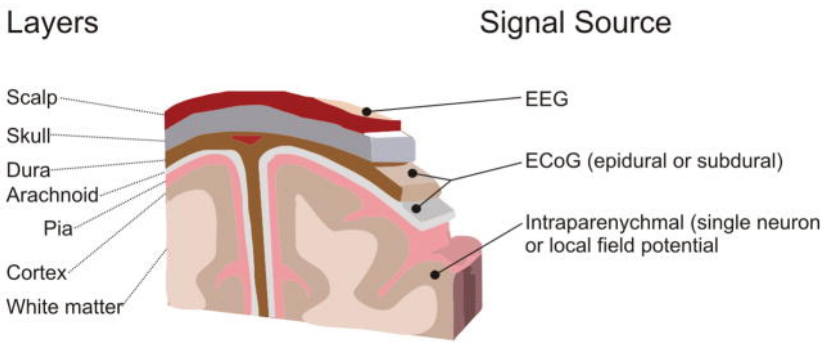

(b)

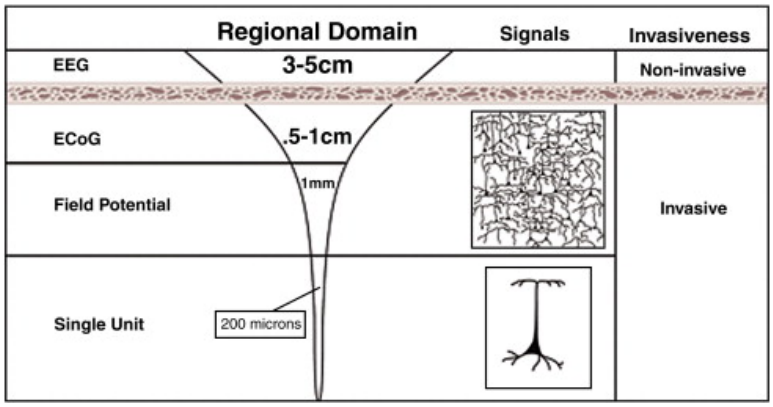

Figure 2.13 EEG, ECoG, local field potential and single unit recording. (a) Signal recording sites. (b) Signal precision versus electrode placement. Although increased precision and isolation of independent degrees of freedom occur with placement of electrodes intracortically, there is also a decrease in signal intensity and increase in noise (Leuthardt et al., 2006, 2009).

2.6.2 ECoG in experimental ischemia

Continuous ECoG monitoring has been advantageous in the experimental ischemia research. Non-convulsive seizures (NCS), polymorphic delta activity (PDA) and periodic lateralized epileptiform discharges (PLEDs) are present in response to focal ischemia (Hartings, Williams, et al., 2003) (Figure 2.14). PDA is a marker of ischemia-reperfusion injury, and it is attenuated by sodium channel antagonists (Williams et al., 2003).

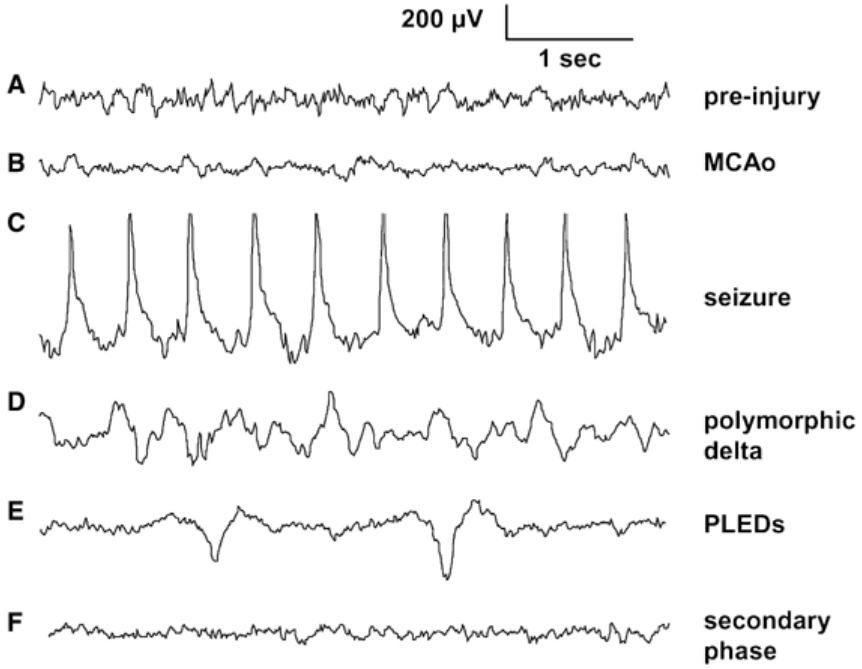

Figure 2.14 Representative ECoG waveforms. (a) Awake, desynchronized activity before MCAo. (b) Amplitude suppression during ischemia. (c) Post-stroke seizure activity. (d) Polymorphic delta activity. (e) PLED. (f) Secondary phase of PID (Hartings et al., 2006).

ECoG topographic mapping provided the spatiotemporal profile of ECoG amplitude recovery (Lu et al., 2001). MCAo produced a significant decrease in the ECoG amplitude in the parietal and temporal cortices. Reperfusion promoted a delayed increase in the ECoG amplitude in the contralesional hemisphere (Figure 2.15).

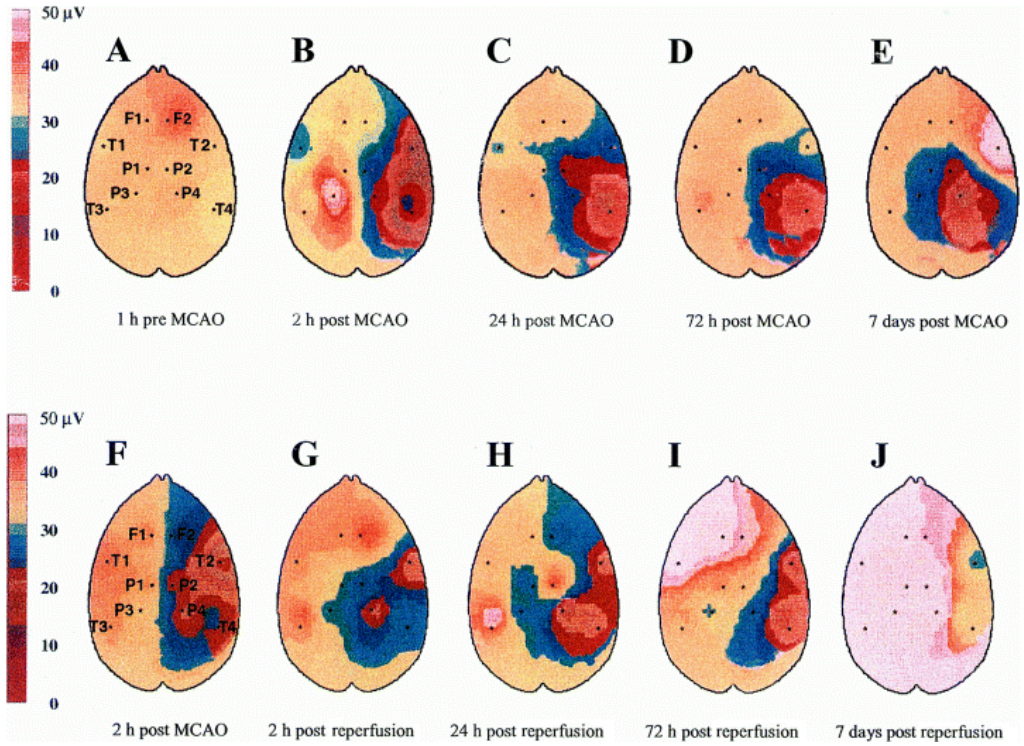

Figure 2.15 Topographic brain mappings of the ECoG amplitude over time after permanent MCAo (a-e) and transient MCAo (f-j). Reperfusion promotes a delayed increase in the amplitude in the contralesional frontal and anterior temporal regions at 72h, which propagates throughout the entire contralesional hemisphere by the day 7 (Lu et al., 2001).

Within the ischemic core, intermittent silence period (loss of all frequencies) was replaced by persistent silence period, suggesting irreversible neural death. Neural activities were preserved in the penumbra with intermittent silence period, suggesting a possibility of neural recovery (Zhang et al., 2007). The neural activities were changed from irregular bursting spikes hours after ischemia to regular synchronized bursting spikes with small amplitude (Zhang et al., 2007). Evoked potential within the penumbra exhibited excitability at acute stroke (Fujioka et al., 2004). Auditory evoke potential shows reduces peak firing rate after focal cortical infarction (Chiganos et al., 2006).

2.6.3 Quantitative EEG (qEEG) in cerebral ischemia

EEG has been used for 30 years to detect risk of cerebral ischemia during carotid surgery (Sharbrough et al., 1973), but it has limited application in acute ischemic stroke (Jordan, 2004). In recent years there has been renewed interest in EEG monitoring for the detection of cerebral ischemia (Friedman and Claassen, 2010). Since the time course of stroke is unpredictable, including sudden worsening, reversal of improvement, seizures, and variable responses to treatments, EEG may therefore serve to complement neuroimaging as a continuous monitor of ongoing ischemia using its high temporal resolution (Friedman and Claassen, 2010). Neuroimaging and bedside neurological assessment are limited when patients are asleep, sedated, paralyzed, or unconscious. On the other hand, real time EEG monitoring will provide timely and physiologically effective surveillance in TIA with a high risk of progressing to stroke (Johnston et al., 2007) and monitoring of secondary stroke extension (Jordan, 2004).

In addition, quantitative EEG (qEEG) is useful for detecting early and subtle ischemic EEG changes (Jordan, 2004). qEEG has provided new insights into post-stroke cerebral pathophysiology and recovery (Finnigan et al., 2007). The brain symmetry index (BSI), a qEEG index based on the difference in mean spectral power for 1-25 Hz between left and right hemispheres, is highly correlated with NIH stroke scale (NIHSS) scores in patients with anterior circulation infarcts (Miche and Dénes, 2004). Besides, the correlation between qEEG and the 30-day NIHSS score is stronger than the correlation between MRI parameters and NIHSS score (Finnigan et

al., 2004). Moreover, a one-time 50% reduction or a sustained 10% decrease in alpha delta ratio can detect delayed ischemia in poor-grade subarachnoid hemorrhage patients (Claassen et al., 2004).

The coupling between EEG and CBF serves the basis for the use of EEG in cerebral ischemia. Fast frequencies are progressively lost and prominent high voltage delta activity appears (Finnigan et al., 2007). When CBF falls below 8-10mL/100g/min, all EEG frequencies are suppressed and irreversible cell death occurs (Jordan, 2004). Therefore, it is theoretically possible to distinguish reversible ischemia from infarction by EEG and use this tool to identify a window of opportunity during which the progression from reversible to permanent damage can be stopped (Friedman and Claassen, 2010).

The scalp EEG recording consists of many electrodes covering the entire head, and it is still unclear how the neural activities in penumbra will be like, i.e. the changes in delta, theta, alpha and beta bands, and their reliability in evaluating post stroke pathophysiology. Besides, the relationship between functional recovery and neural activity recovery has not been studied quantitatively in experimental ischemia, since most of the previous studies were limited to the EEG polygraphic recording and power spectra analysis. It is important to investigate the neural activities from acute to chronic phase by using a rat model of focal ischemia, and correlated ECoG with infarct growth and functional recovery.

CHAPTER 3 METHODOLOGY

The design of this study has been divided into three parts: (1) histological analysis of infarct growth and location of penumbra by TTC staining; (2) ECoG analysis after focal cerebral ischemia; (3) functional evaluation (Figure 3.1). They are conducted at acute, subacute and chronic phases after MCAo.

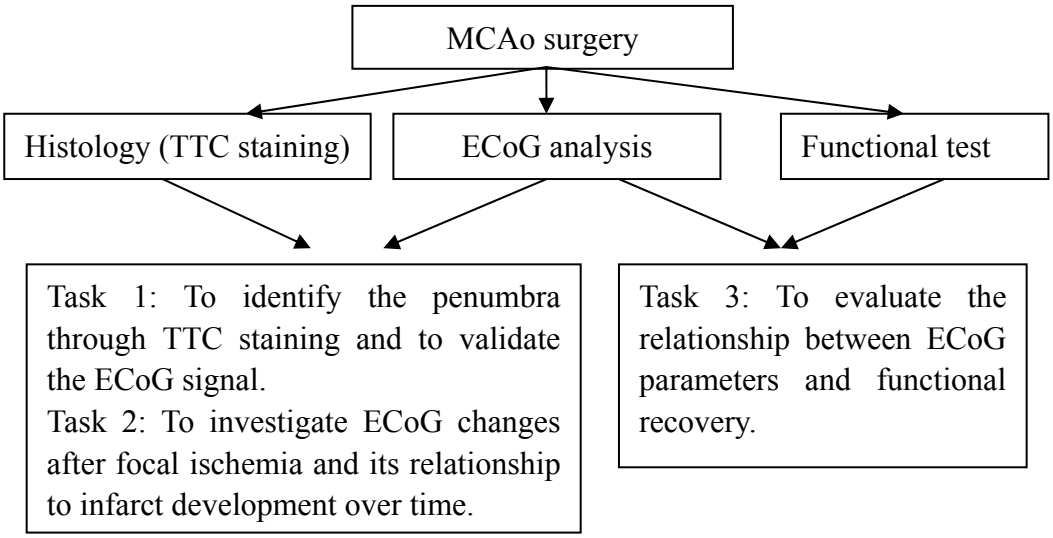

Figure 3.1 Structure of the study

All the experimental procedures were carried out in accordance with the National Institute of Health Guide for the Care and Use of Laboratory Animals. The experimental protocol was approved by Department of Health in Hong Kong and Animal Subjects Ethics Sub-Committee (ASESC) of the Hong Kong Polytechnic University.

3.1 MCAo surgery

Male Sprague Dawley rats with body weight 300-320g (8 weeks old) were housed individually during 12h day/night cycle with free access to water and food in a

temperature controlled environment at 20°. Rat was anaesthetized with chloral hydrate (0.4mg/kg). Ischemia was induced in the right hemisphere of rat brain using intraluminal filament method as described previously (Koizumi et al., 1986; Ke et al., 2011). The right carotid region was exposed through a midline cervical incision (about 20mm). The right CCA and right ECA were isolated from the surrounding tissue and ligated with a 6-0 suture. A 4-0 nylon suture coated with poly-l-lysine, with its tip shaped round, was inserted into the right ICA and advanced to a point approximately 17-20mm distal to the bifurcation of ECA and ICA where the proximal segment of the ACA starts, thereby occluding the origin of the MCA (Figure 3.2). Reperfusion was made by slow extraction of the nylon suture at 90 minutes after occlusion. During the surgery, rat's core temperature will be maintained by a heating lamp. Enrofloxacin was injected intramuscularly (2.5mg/kg) for prophylaxis after MCAo. The MCAo surgery was supported by my research colleague (Ke Zheng) in this study, because she was experienced to do this surgery. After the MCAo, rats with stroke symptoms were selected for the experiment.

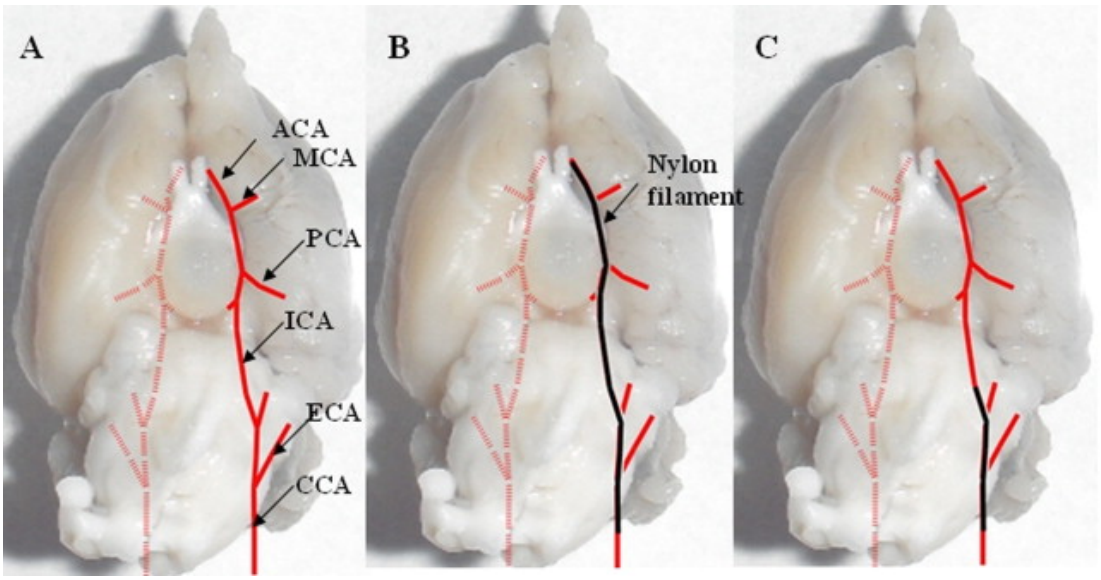

Figure 3.2 MCAo surgical procedures. (A) Schematic illustration of the cerebral arteries in the rats. Anterior cerebral artery (ACA), middle cerebral artery (MCA), posterior cerebral artery (PCA), internal carotid artery (ICA), external carotid artery (ECA), common carotid artery (CCA). (B) Schematic illustration of MCAo by nylon suture (black). (C) Schematic illustration of the sham operations

3.2 Histological method

Rat brain was carefully removed and cut into 2mm coronal sections using a brain matrix (RBM-4000C; ASI Instruments Inc., Houston, Texas, USA) (Figure 3.3a). The brain slices were stained with TTC (Sigma-Aldrich Co., St. Louis, Missouri, USA) in a phosphate buffered solution (PBS) at 37° for 30 minutes and then fixed in 10% formaldehyde overnight. TTC staining could easily differentiate viable tissue from infarction macroscopically. Viable brain tissue was stained red (Figure 3.3b) (Liu et al., 2009). TTC stained brain slices were photographed with a digital camera (Casio EX-Z2000, Japan).

(a) (b)

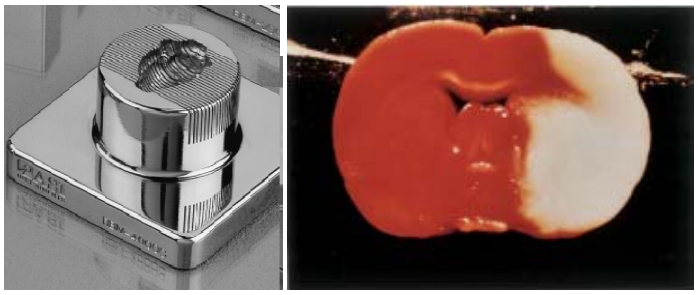

Figure 3.3 Histological method. (a) Brain matrix for brain coronal section. (b) A TTC stained coronal section (Li et al., 1998).

3.3 ECoG analysis

3.3.1 ECoG electrodes implantation

Rat was anaesthetized with chloral hydrate (0.4mg/kg) and placed on a stereotaxic system (SAS-4100, ASI Instruments Inc., Houston, Texas, USA) (Figure 3.4a). Blur holes were drilled on the skull to expose the dura. Two stainless steel electrodes with 1.0mm in diameter were placed on surface of dura covering bilateral motor cortex (M1) and hindlimb sensory cortex (S1HL) (Li et al., 1998). According to the rat brain atlas, M1 and S1HL were located at posterior 1mm to bregma and 2mm lateral to midline (Paxinos and Watson, 2007) (Figure 3.4b). Similar electrode location was reported by previous studies using continuous EEG to evaluate drug effects on focal cerebral ischemia (Tortella et al., 1999; Lu et al., 2001; Hartings, Williams, et al., 2003; Kelly et al., 2006). Reference electrode was implanted over the occipital cortex. All the electrodes were soldered to a multipin connector (Figure 3.4c), which was secured on the skull by dental cement (Figure 3.4d).

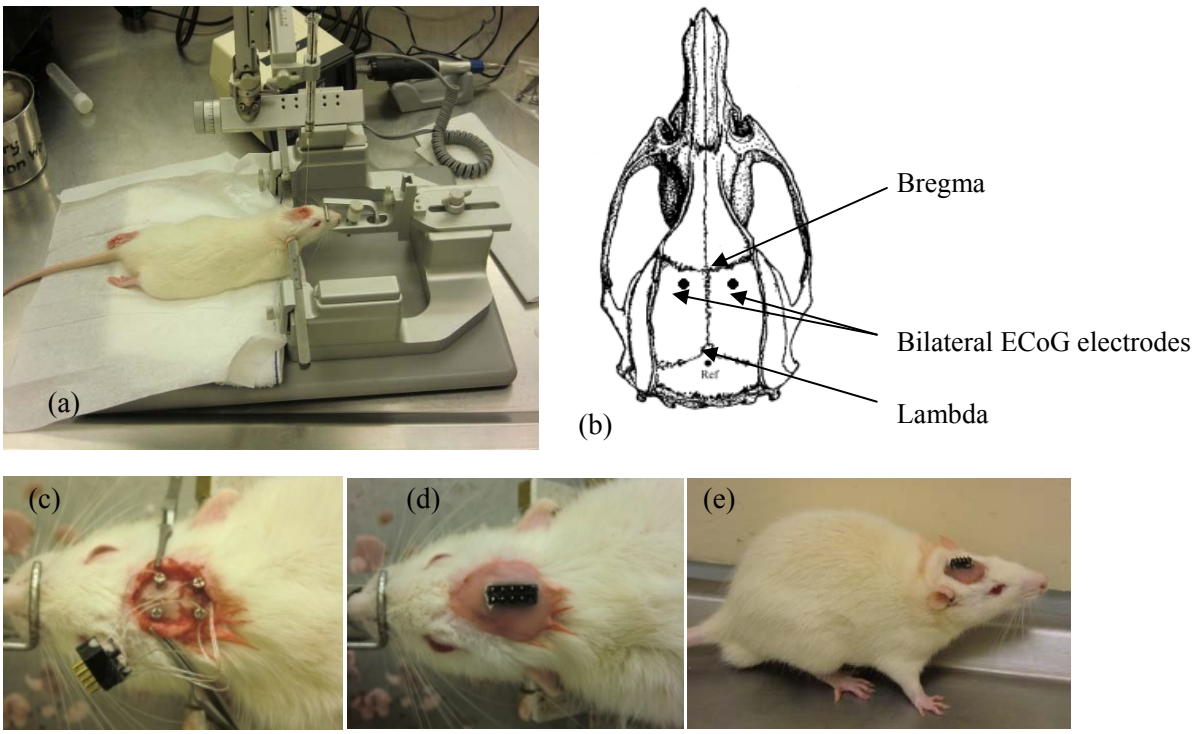

Figure 3.4 ECoG electrodes implant surgery. (a) Rat is fixed on the stereotaxic apparatus. (b) ECoG electrodes placement. (c) Electrodes wired to multipin connector. (d) Multipin connector fixed on the skull with dental cement. (e) Rat revives from anesthesia.

3.3.2 ECoG recording protocol

ECoG were collected from pre-stroke phase (0h), acute phase (3h and 6h), subacute phase (24h, 48h and 72h) to chronic phase (96h, 120h, 144h and 168h) (Soltanian-Zadeh et al., 2003; Xu et al., 2006). ECoG signal was high pass filtered at 0.3Hz and amplified 100 times by an pre-amplifier (SR560, Stanford research, USA). ECoG was digitalized by a data acquisition system (RM6240B, Chengdu Instrument, China) with a sampling frequency of 200Hz and stored for offline analysis (Figure 3.5).

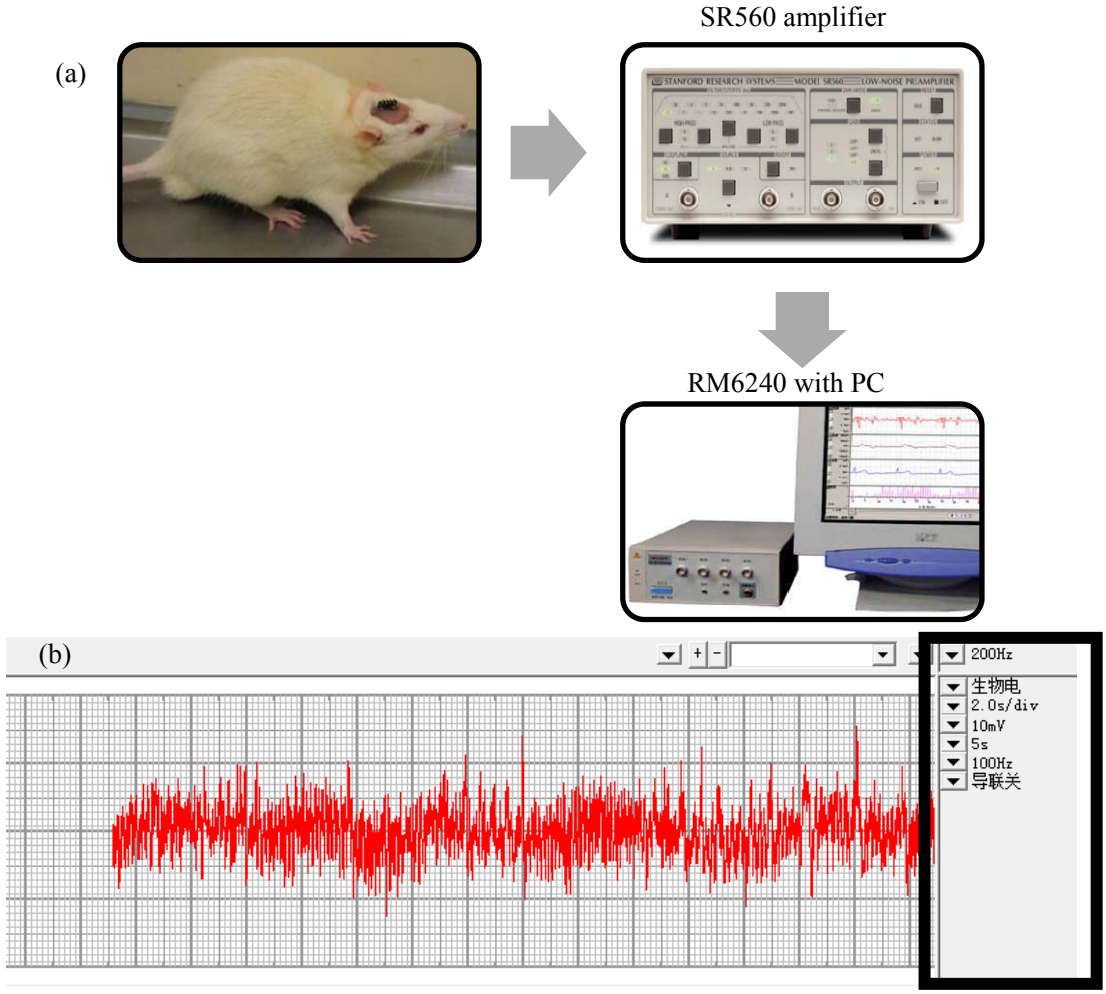

Figure 3.5 ECoG signal recording. (a) ECoG signal flow chart (b) ECoG recorded by RM6240. Recording parameters: sampling frequency: 200Hz, voltage: +/-10mV, time scale: 2s/div, time coefficient: 5s, low pass filter cut off frequency: 100Hz.

3.3.3 ECoG spectral analysis using autoregressive model

Though ECoG is non-stationary and time varying, short-time ECoG can be considered as a stationary process, and its power spectrum can be estimated by the autoregressive (AR) model. AR model can be described by the equation (1), where a_i is the model coefficient, $x(n)$ is the ECoG time series and $w(n)$ is white noise.

$$x(n) = a_1 x(n-1) + a_2 x(n-2) + a_3 x(n-3) + ...a_p x(n-p) + w(n) \quad (1)$$

The AR power spectrum is given by

$$X(w) = \frac{W(w)T}{\left| \prod_{k=1}^{p} (e^{-jwT} - P_k) \right|^2} \quad (2)$$

Where P_k are the complex poles of $X(w)$. Therefore, at the frequencies satisfying $e^{-jw_kT} = P_k$, there are corresponding peaks in the spectrum. The peaks in the power spectrum, namely dominant frequencies, are usually of interest in quantitative analysis (Thakor and Tong, 2004).

In the AR model, a smaller p would induce smooth peak and a larger p would yield false peak (Thakor and Tong, 2004). Selection of p was based on Akaike's information criteria (AIC, equation (3)), where e was the error of the model.

$$AIC(p) = N \log(e^2) + 2p \quad (3)$$

The length of ECoG clip was optimized to minimize error. Frequency analysis was performed from 3.3s ECoG clip, since ECoG clip of similar duration was reported in previous studies (Murri et al., 1998). Artifact detection was based on visual assessment of raw ECoG. Based on equation (2), ECoG power spectrum density (PSD) could be calculated with respect to delta band (0.5-4Hz), theta band (4-8Hz), alpha band (8-13Hz) and beta band (13-30Hz).

3.3.4 Alpha to delta ratio

Alpha to delta ratio (ADR) was the ratio between alpha band power and delta band power. It was applied to investigate the sequential changes in ECoG after ischemia (equation (4)). An increase in ADR was regarded as brain activity changing from slow oscillation to faster oscillation.

$$\text{ADR} = \frac{\text{Alpha} \quad (8 - 13\ \text{Hz})}{\text{Delta} \quad (1 - 4\,\text{Hz})} \tag{4}$$

3.3.5 Peak power variability

ECoG signals demonstrate inherent variability with changes in the peak power within each frequency band. Since the spectral power might have different values depending on whether it was measured in the beginning or in the end of the recording, the peak power at different frequencies might contain certain trends over the course (Maltez et al., 2004). Therefore, peak power variability is monitored from pre-stroke phase to chronic phase. In this study, 80 ECoG clips were chosen from ECoG recording. Alpha, beta and delta peak powers were calculated from each 3.3s ECoG and displayed in separate histograms. Particularly, Vespa et al. reported that alpha variability could indicate delayed ischemia in patients with vasospasm (Vespa et al., 1997) (Figure 3.6).

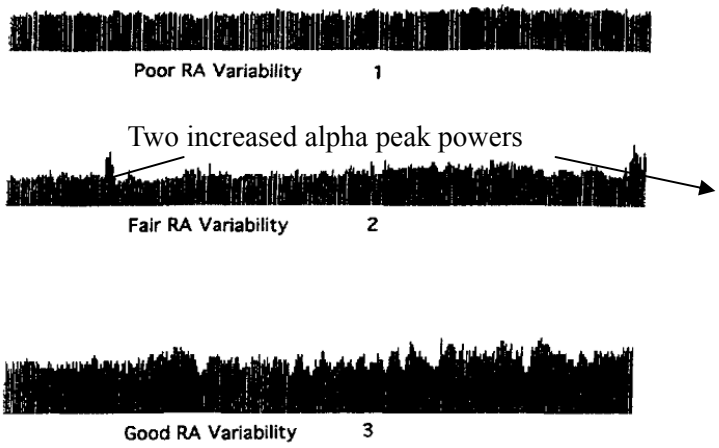

Figure 3.6 Alpha peak power variability. Score 1: poor alpha variability. Alpha peak powers keep constant over time; score 2: fair alpha variability. Notice two elevated peaks in the time course, while the majority of alpha peak powers keep constant; score 3: good alpha variability. Alpha peak power is changing from time to time.

3.4 Functional evaluation

Functional outcome is necessary to assess the consequences of stroke (Virley et al., 2000). This study used Longa's test, De Ryck's test and beam walking test to evaluate post-stroke functional outcome. The Longa's neurological score roughly indicated the neurological status, i.e. infarction severity (Figure 3.7). De Ryck's test evaluated the forelimb function, and it excluded a natural compensatory strategy to learn to rely on the nonparetic limb (Metz et al., 2005). Beam walking test evaluated the motor coordination and balance, particular focusing on the hindlimb function. Each test was performed three times to get an average score.

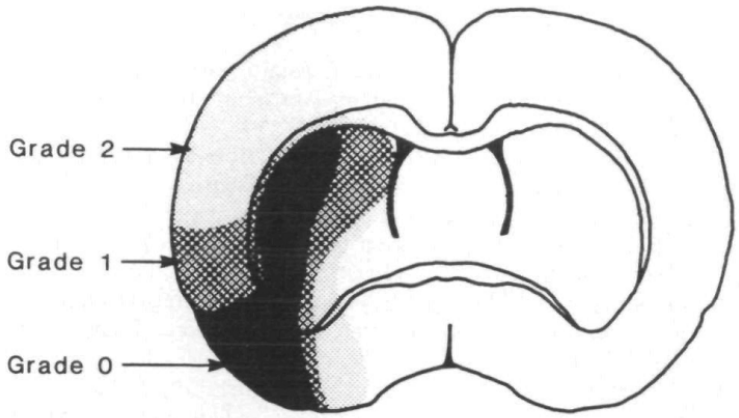

Figure 3.7 Relationship between Infarct size and neurological score (Bederson, Pitts, Tsuji, et al., 1986)

3.4.1 Longa's test

Neurological deficits were evaluated on Longa's scale after MCAo (Longa et al., 1989). Longa's scale was used as rat selection criteria in this study (Table 3.1). Rats scored 1 to 2 in Longa's neurological assessment were selected for the experiment.

Table 3.1 Longa's neurological scale (Longa et al., 1989)

Scores	Longa's scale
0	No neurologic deficit
1	Failure to fully extend forepaw on the affected side
2	Circling to the affected side
3	Falling to the affected side
4	Did not walk spontaneously and had a depressed level of consciousness

3.4.2 De Ryck's test

De Ryck's test evaluated the sensorimotor function after MCAo. Briefly, postural reflex, visual placing in the forward and sideways directions, tactile placing of the dorsal and lateral paw surfaces, and proprioceptive placing were tested in the 8 subtasks (De Ryck et al., 1989). Six subtasks tested the forelimb function while the left two subtasks tested the hindlimb function (Figure 3.8). These 8 tasks are described as follows:

1. The rat was suspended 10 cm over a table. Normal rats could stretch their ipsilesional forelimbs towards the table.
2. Forelimb placement of the rat when facing a table edge. A normal rat could place both forepaws on the table top.
3. By keeping the head upward in a 45 angle, the rat was prohibited from seeing the table or contacting it with its whisker.
4. The rats were placed along the table edge to check for lateral placement of the forelimb and hindlimb (two subtasks).
5. The rat was positioned towards the table, with the limbs just over the edge. By gently pushing the rat body towards the side of the table, the injured forelimb and

hindlimb slipped off the edge (two subtasks).

6. The forelimbs were placed on the edge of the table and the rat was gently pushed from behind toward the edge. Stroke rats could not keep their grip and the injured forelimb slipped off the edge.

Each task were scored as follows: 2 points, the rat performed normally; 1 point, the rat performed with a delay (2s) and/or incompletely; and 0 points, the rat did not perform normally. The behavioral deficit was calculated as the sum of the scores of the individual tests ranging from 0 (maximum deficit) to 16 (no deficit).

Figure 3.8 De Ryck's sensorimotor for rat with focal ischemia. (a) rat cannot use its affected forelimb (circled) to touch the ground; (b) rat could not place its affected forelimb (circled) on the table edge when the head was tilted; (c) the rat could not place affected limb (circled) on the table edge simultaneously as unaffected limb when facing the table edge; (d) the rat could not place affected forelimb & hindlimb (circled) on the table edge when it was placed near the table edge; (e) the rat could not place its affected forelimb & hindlimb (circled) on the table edge when the rat was pushed laterally; (f) rat could not use its affected limb (circled) to grasp the edge when pushed forward.

3.4.3 Beam walking test

The beam walking test was used to assess hindlimb motor coordination and integration of movement. This test involves scoring foot slips during transverse of a 2.5 cm wide, 122 cm long beam (Feeney et al., 1982). The beam was elevated at 42 cm from the ground and placed horizontally with the home cage placed at the target end. The rats were placed at the one end of the beam, and their foot slips were counted during their walk to their home cage. Rats were tested from day 1 to day 7 after MCAo. The average score of 3 transverses was recorded. The maximal score is 6, meaning that there was no foot slip during the transverse, and the minimal score is 0, meaning that the rat could not maintain a balance on the beam. The detailed scoring system of beam walking test was described in Table 3.2.

Table 3.2 Beam walking criteria (Jolkkonen et al., 2000)

Beam walking score	Description
0	The rat is not able to maintain balance and falls down from the beam
1	The rat is unable to traverse the beam but remains perched on the beam
2	The rat falls down while walking
3	The rat can traverse the beam by dragging foot on the affected side
4	The rat traverses the beam with more than 50% foot slips
5	The rat crosses the beam with less than 50% foot slips
6	The rat crosses the beam with no foot slips

3.5 Statistical analysis

According to previous papers studying ECoG activities in rat MCAo model, 8-12 rats for each group were used in statistical analysis (Lu et al., 2001; Hartings, Rolli, et al., 2003; Chiganos et al., 2006). In this study, statistical analysis was performed with commercially available statistical software (SPSS version16.0, SPSS Inc, Chicago,

IL, USA). ADRs, De Ryck's scores and beam walking scores were expressed as mean ± standard deviation. They were compared between the time points from 48h to 168h with the 24h post stroke by paired t-test to evaluate the sensorimotor functional recovery. The Pearson's correlation is used to find a correlation between two continuous variables (ADR and De Ryck's score). The value for a Pearson's can fall between 0 (no correlation) and 1 (perfect correlation). Generally, correlations above 0.8 are considered high. The significant level is to test whether the two variables are statistically correlated. $p<0.05$ is considered as statistical significant in this study.

CHAPTER 4 RESULTS

60 male SD rats with body weight 300-320g (8-weeks old) underwent MCAo. 28 rats showed no motor deficits, and 8 rats died post-operatively possibly due to severe stroke. The rats with sensorimotor deficits were divided into three groups: a histology group (n=8), a reliability test group for ECoG signal setup (n=4) and an ECoG recording group (n=12). In the histology group, 8 rats were selected for TTC staining at 3h (n=2), 6h (n=2), 24h (n=2) and 72h (n=2). 2 rats from the ECoG recording group were used in the TTC staining at 168h. In the ECoG recording group, the data from 4 rats whose electrodes dropped during 7-day recording was excluded. As a result, the 8 rats left were included in the final statistical analysis.

4.1 Histology

Infarct was limited to the striatum and the parietal cortex at 3h, and it did not affect M1 and S1HL. The infarct developed most rapidly from 6h to 24h, and it gradually moved from paritel cortex to M1 and S1HL. The infarct would mature over 72h and did not subsequently expand (Figure 4.1a). The internal capsule (IC), caudate putamen (CPu), globus pallidus (GP), and parietal cortex lacked of TTC staining (white). M1/S1HL was identified as the infarct penumbra (Figure 4.1b), which was also consistent with the location of ECoG electrode.

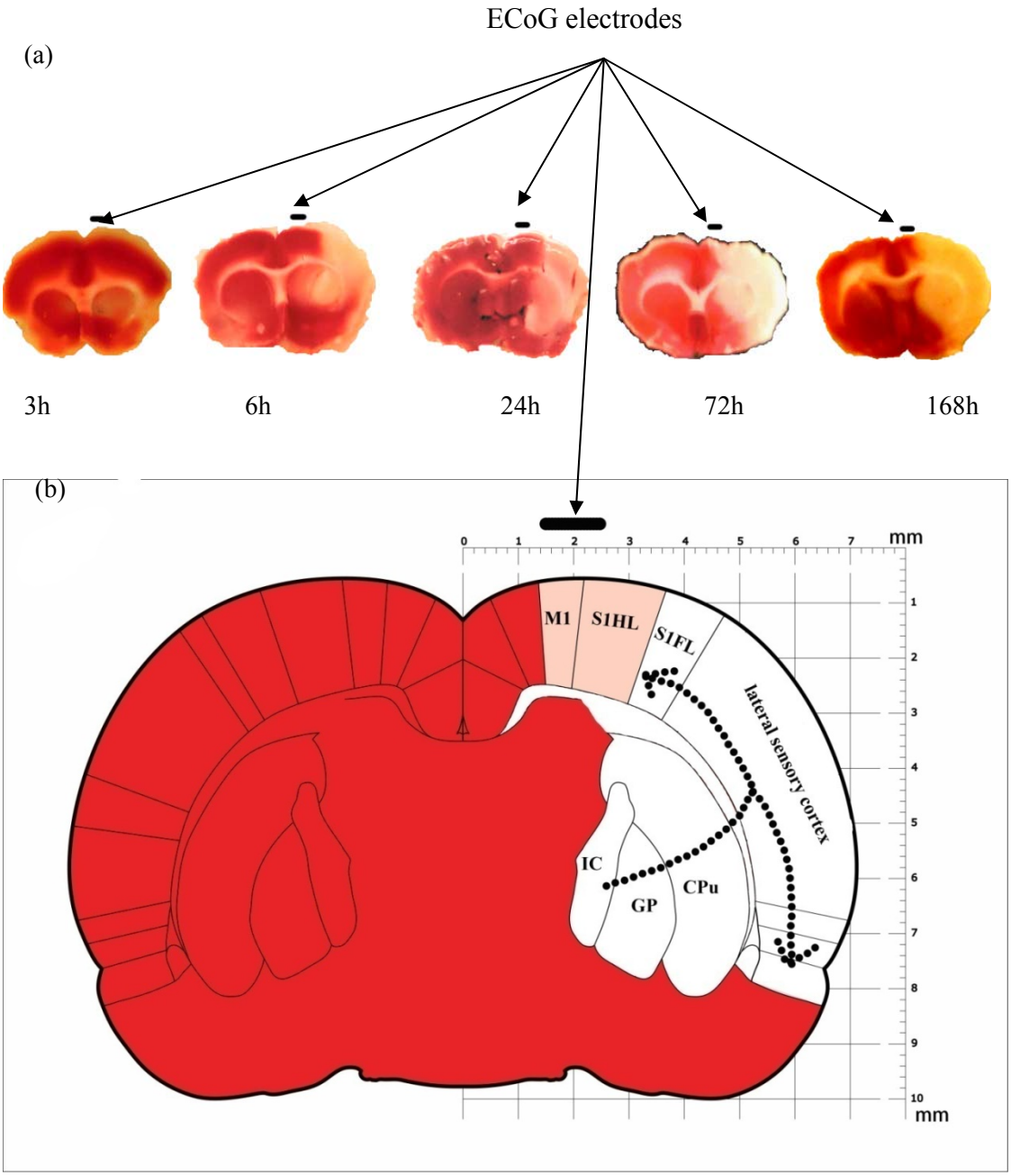

Figure 4.1 Infarct development process. (a) Brain infarction revealed by TTC staining at different time points. The black label marks the location of the ECoG electrode. (b) An enlarged picture shows the brain structure affected by ischemia. The course of infarct development is marked with a dashed black arrow.

4.2 Crosstalk from ECG

It has been reported that electrical field of the heart (ECG) propagates throughout the

body and introduce artifact in EEG recordings which leads to incorrect interpretation of monitoring result (Park et al., 2002), this study tested whether there was ECG interference in the ECoG recordings, and the results showed no sign of ECG interference in the ECoG recording (Figure 4.2).

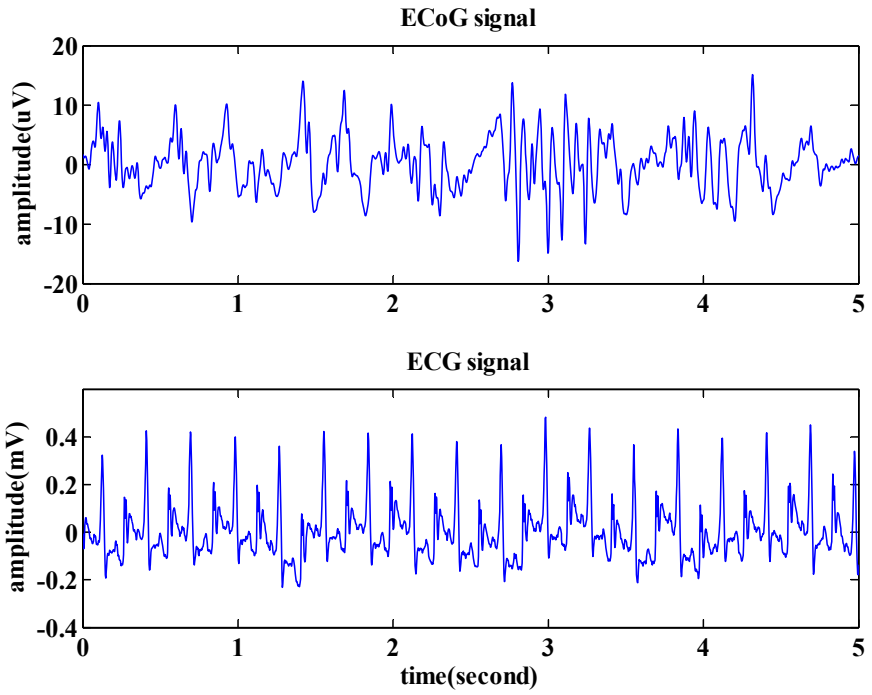

Figure 4.2 Simultaneous recording of ECoG and ECG. No statistically correlation was found between ECoG and ECG ($r=0.0203$, $p>0.05$).

Based on Akaike information criteria (Sectioin 3.3), AR model ($p=24$) was used to calculate ECoG power spectrum density (PSD). The PSDs of non-ischemic ECoG and ischemic ECoG are shown in Figure 4.3. Power spectrum was severely distorted after brain ischemia, with 3-4 fold increase in low frequency peak power (Figure 4.3c, Figure 4.3d).

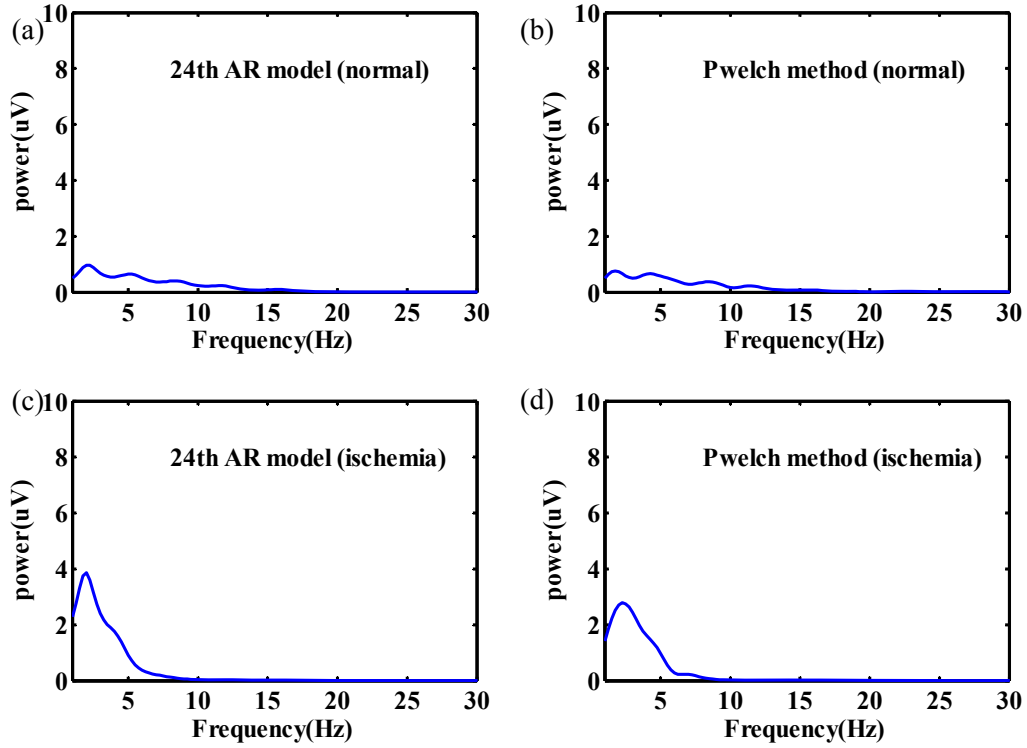

Figure 4.3 Non-ischemic and ischemic ECoG power spectrum. (a) Pre-stroke ECoG PSD estimated by AR model. (b) Pre-stroke ECoG PSD estimated by Welch's method. (c) Ischemic ECoG PSD estimated by AR model. (d) Ischemic ECoG PSD estimated by Welch's method.

4.3 ECoG Power spectra estimation

4.3.1 Pre-stroke phase

Pre-stroke ECoG was irregular and not synchronous (Figure 4.4a). Delta, theta, alpha and beta powers constituted 45%, 40%, 12% and 3% of the total ECoG power in the global frequency band (1-30 Hz), respectively (Figure 4.4b).

4.3.2 Acute stroke phase

In the acute stroke phase, delta power was enhanced and accompanied by compensated decreases in theta, alpha, and beta power, showing the effects of ischemia. Fast background activity (alpha/beta) was still preserved in the ECoG

wave (Figure 4.4c). Two large peaks within 1-5 Hz frequency range were observed (Figure 4.4d). The balance of the delta, theta, alpha and beta powers was redistributed to 85%, 7%, 5%, and 3% of the total power.

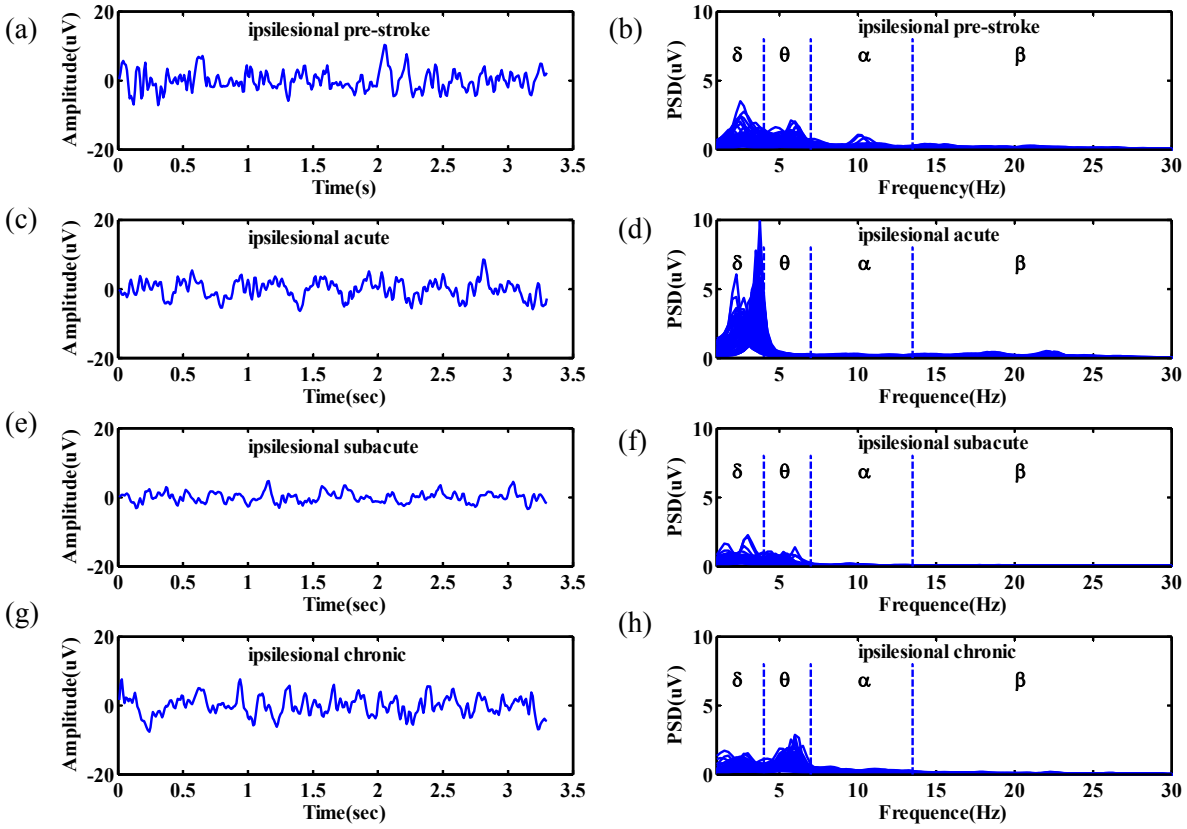

Figure 4.4 ECoG and its power spectrum in the pre-stroke (a, b), acute stroke (c, d), subacute stroke (e, f) and chronic stroke phases (g, f).

The ECoG amplitude decreased to 44.3±5.9% of the pre-stroke level after MCAo and recovered to 64.4±4.4% of the pre-stroke level after reperfusion (Figure 4.5).

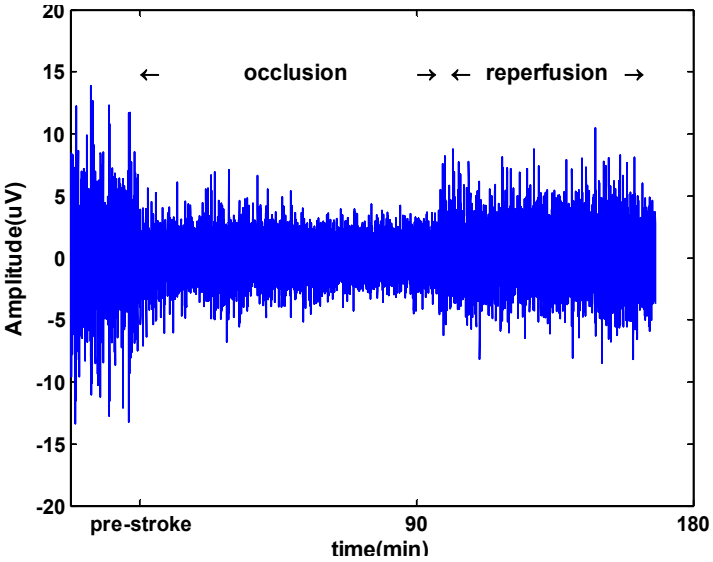

Figure 4.5 ECoG amplitude change after MCAo

4.3.3 Subacute stroke phase

In the subacute phase, the delta and theta power began to recover. The delta power generally returned to the pre-stroke level by 24-48h. Reduced fast activity was found in the ipsilesional side (Figure 4.4e) and a loss of alpha/beta power was found in the corresponding ECoG spectrum (Figure 4.4f). The alpha/beta power was gradually reduced to 30-40% of the pre-stroke level by 72h. For the contralesional side, the alpha power remained unchanged (Figure 4.6a), and the beta power first increased before returning to the pre-stroke level at 72h (Figure 4.6b).

4.3.4 Chronic stroke phase

In the chronic phase, the ECoG power spectrum began to recover during the chronic phase (Figure 4.4h), and a delayed increase in alpha/beta power was observed. The alpha power returned to 90% of the pre-stroke level after 168h (Figure 4.6a), but the beta power was only restored to 50% of the pre-stroke level in the ipsilesional side. In the contralesional side, the beta power began to increase from 96h (Figure 4.6b).

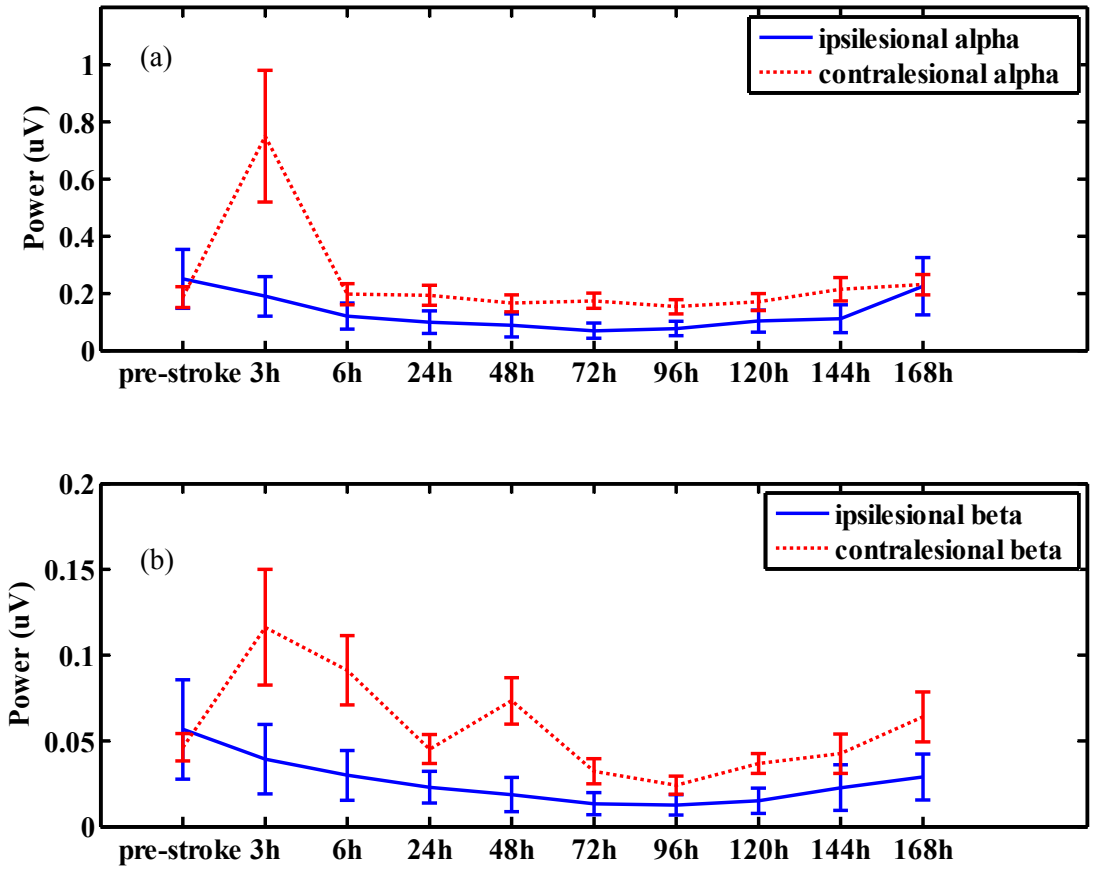

Figure 4.6 Alpha (a) and beta band (b) power trend over time.

4.4 Alpha to delta ratio (ADR)

ADRs in early ischemia (0.0390 ± 0.0109) dropped below 20% of baseline and gradually recovered from the subacute phase to the chronic phase. ADRs at 96h, 120h, 144h and 168h were significantly larger than ADRs at 24h ($p<0.05$). If the ADR threshold of ADR was set at 0.1300 (50% of pre-stroke ADR), subacute stroke ADRs could be separated from chronic stroke ADRs with 85.7% accuracy. The ADRs from 24h to 72h was below 0.1300, and the ADRs from 96h to 144h were between 0.1300 and 0.2353 (pre-stroke ADR). The ADR at 168h (0.2248±0.0806) was almost at the same level as the pre-stroke ADR (Figure 4.7).

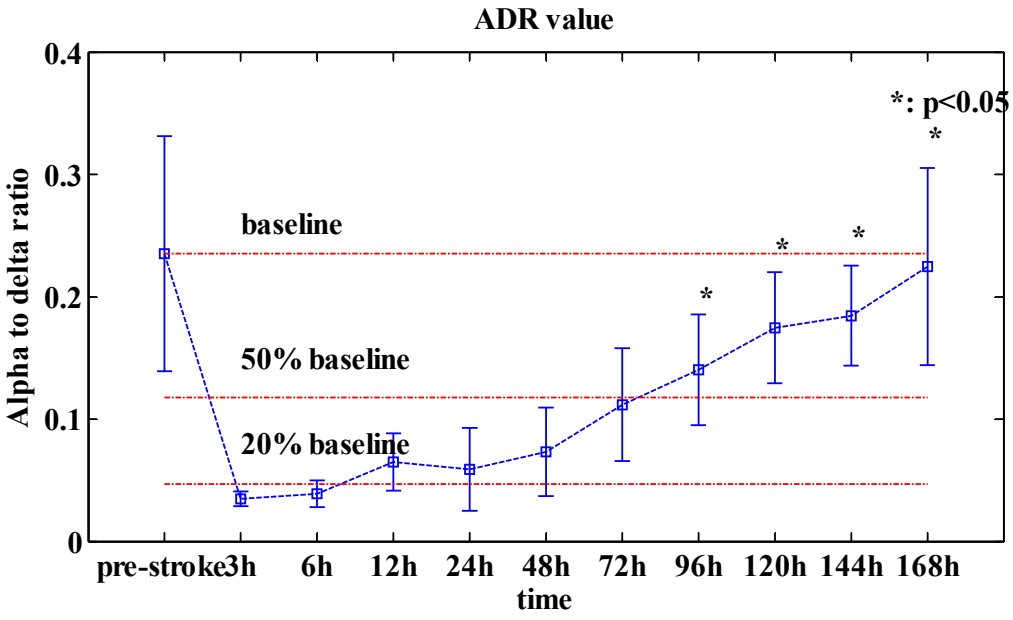

Figure 4.7 Changes in ADRs after ischemia. The ADRs from 3h to 6h are below 20% of the baseline level, and the ADRs from 24h to 72h are below 50% of the baseline level.

4.5 Peak power variability

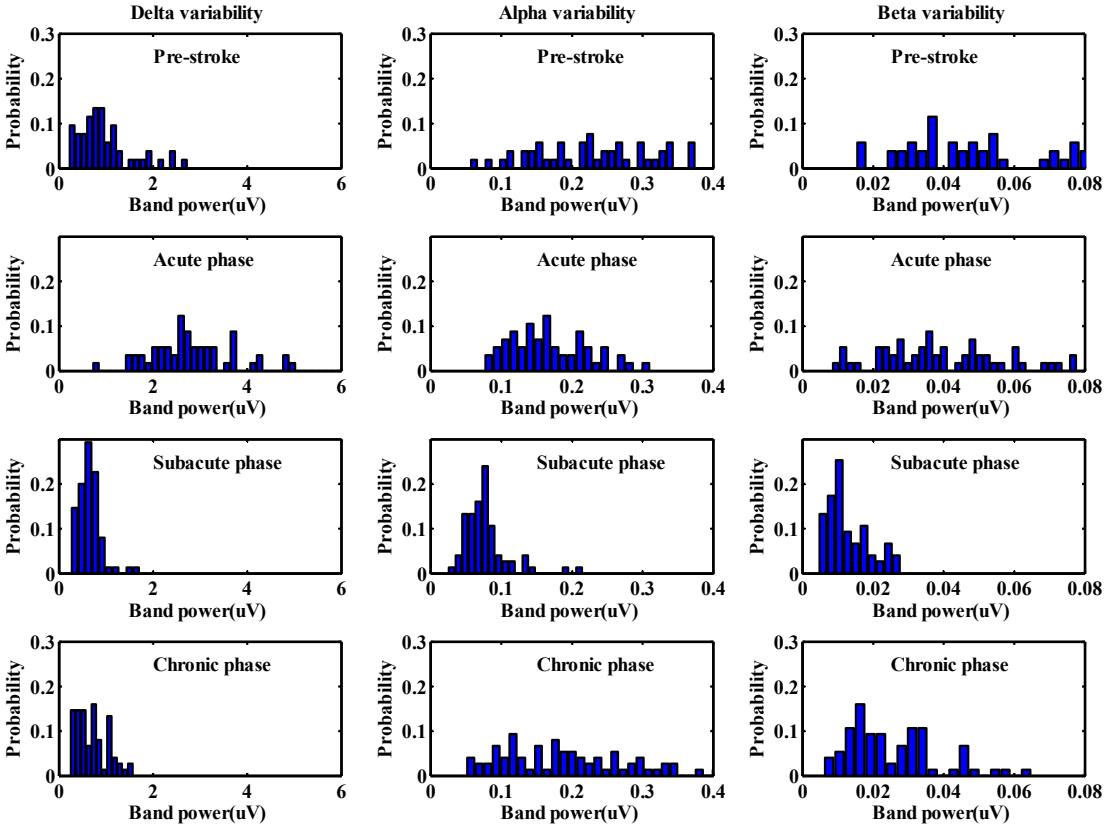

Figure 4.8 Delta, alpha and beta peak power variability

The pre-stroke delta peak power ranged from 0-2uV, mostly around 1uV (with the highest occurrence probability). In the acute phase, the delta peak power distribution ranged from 1uV to 6uV, and most of the delta power exceeded 2uV. In the subacute and chronic phases, the delta peak power distribution returned to the pre-stroke distribution, and its peak power was most likely to be 1uV (Figure 4.8 left column).

The pre-stroke alpha peak power varied from 0uV to 0.4uV, mostly around 0.2uV. The alpha peak power variability gradually decreased to the 0-0.2uV range, with 0.1uV power occurring most frequently in the subacute phase. In the chronic phase the alpha peak power distribution returned to the pre-stroke distribution (Figure 4.8 middle column).

The pre-stroke beta peak power varied from 0uV to 0.08uV, mostly around 0.04uV. The beta peak power variability gradually decreased to the 0-0.02uV range, with 0.01uV power occurring most frequently in the subacute phase. The beta peak power distribution could not fully return to the pre-stroke distribution (0-0.06uV) in the chronic phase (Figure 4.8 right column).

4.6 Correlation between ECoG and functional recovery

The rats' sensorimotor function recovery was shown in Figure 4.9a. The deficits were observed as early as 6h after ischemia. The De Ryck's scores reached their minimum at 24h (3.0±1.1), and gradually recovered afterward. The De Ryck's scores at 96h (4.8±1.1), 120h (5.8±1.1), 144h (6.5±1.3) and 168h (7.5±1.7) were significantly different from the score at 24h ($p<0.05$). For all of the rats, the sensorimotor function could not fully recover after 168h, and they still exhibited sensorimotor deficits.

The beam walking scores are shown in Figure 4.9b. As with the De Ryck's score, the beam walking scores reached the minimum at 24h after ischemia (2.0±1.5). The scores at 48h (2.9±1.8), 72h (3.3±1.9), 96h (3.6±1.9), 120h (4.1±1.5), 144h (4.5±1.4), and 168h (4.9±1.5) were significantly different from the score at 24h ($p<0.05$). The beam walking scores recovered much faster than the De Ryck's scores. Four rats (50%) scored 6 and two rats (25%) scored 5 at the end of the experiment (168h).

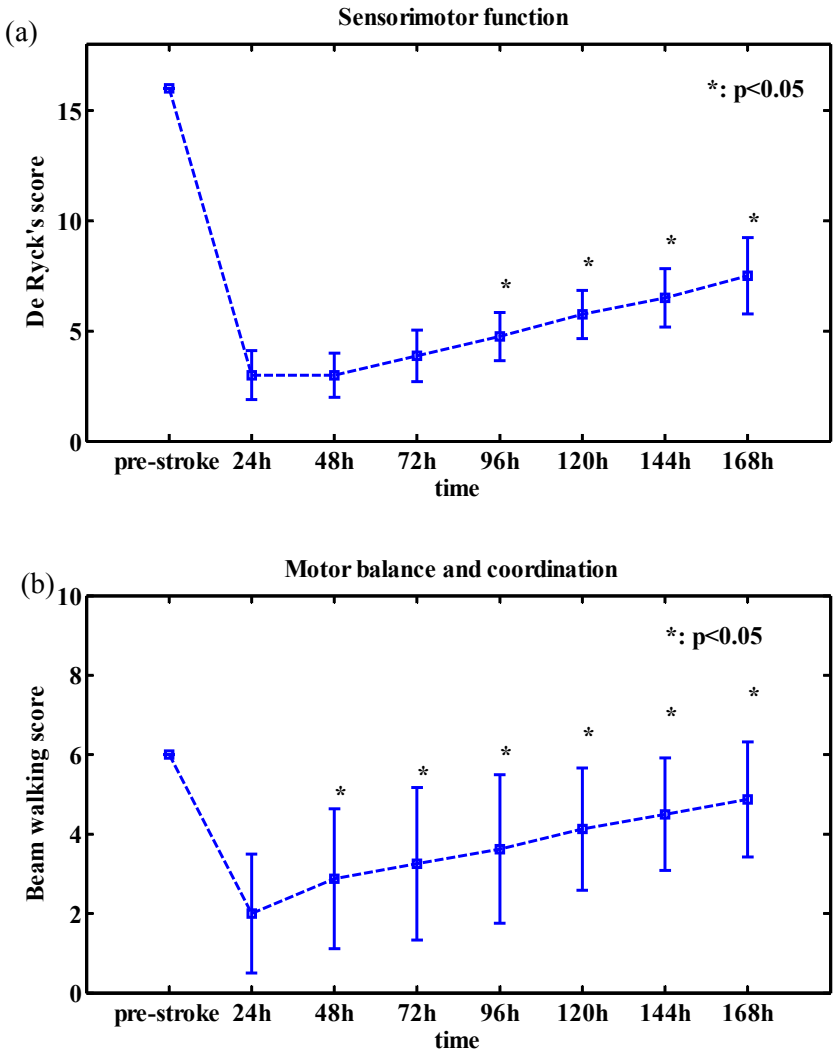

Figure 4.9 Recovery of sensorimotor function and motor coordination. (a) The De Ryck's scores from 96h to168h are significantly different from the score at 24h. (b) Significant improvement in the beam walking scores from 48h.

The ADRs and De Ryck's scores fitted the linear regression model ($p<0.01$) within the 24h-168h time window (Figure 4.10a). The recovery of De Ryck's scores was highly correlated with the restoration of ADRs ($r=0.9895$, $p<0.05$) (Figure 4.10b).

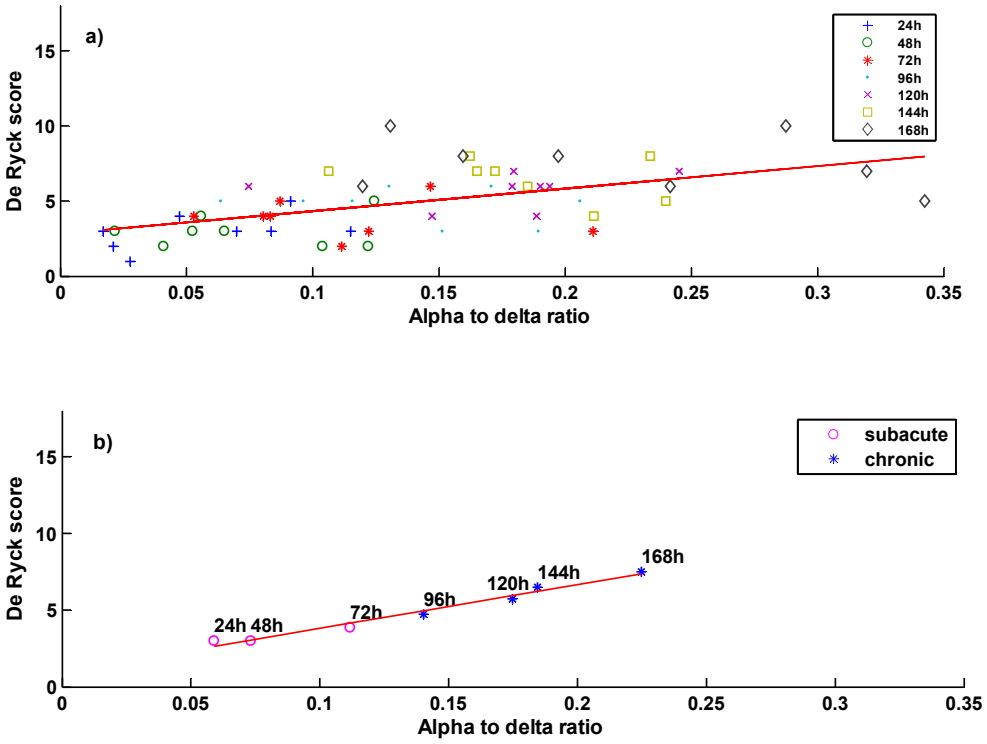

Figure 4.10 Correlation between the De Ryck's scores and ADRs. (a) Scatter plot of the De Ryck's scores and ADRs. (b) Positive correlation between the De Ryck's scores (average of 8 rats' data) and ADRs (average of 8 rats' data) within 24h-168h.

CHAPTER 5 DISCUSSION

The present study established a focal cerebral ischemia model with ECoG recording and investigated neural activities from free-behaving rats. The results showed that ECoG could provide information on post-stroke pathophysiology. Brain infarction gradually developed from the striatum to the cortex after 90-min MCAo, and the changes in the ECoG delta, alpha and beta bands matched well with the course of infarct development. As for quantitative ECoG parameters, the improvement in ADRs was highly correlated with sensorimotor functional recovery. Decreased alpha/beta variability might be another indicator of reversible neural dysfunction.

Compared to previous studies using a focal cerebral ischemia model, the present study has several advantages. First, quantitative ECoG provided complementary information by studying different ECoG parameters after stroke. The use of ADR reduced the inter-subject variance, and allowed comparison between stroke rats. An ADR threshold (50% of pre-stroke ADR) was able to indicate delayed ischemia for a longer time window (i.e., up to 72h) than in previous studies (i.e., PIDs were limited to 24h). Second, the experiment simulated clinical conditions by recording neural activities in awake, freely-moving animals, thereby avoided the bias from anesthesia and restraint. Third, ECoG recordings were performed repetitively on each rat, and pre-stroke baseline recordings could be used for intra-subject comparisons.

5.1 Infarct development

The suture MCAo model produced an infarct in the basal ganglia and dorsolateral

cortex overlying the striatum. The basal ganglia consistently suffered severe ischemia whereas the cerebral cortex exhibited a gradient of decreased blood flow from the periphery to the central parts of dorsolateral cortex (Figure 5.1). Although the precise localization of penumbra and core depends on the animal strain and the method of occlusion (Hossmann, 2008), 2-3mm from the midline is generally considered as the penumbra (Figure 4.1).

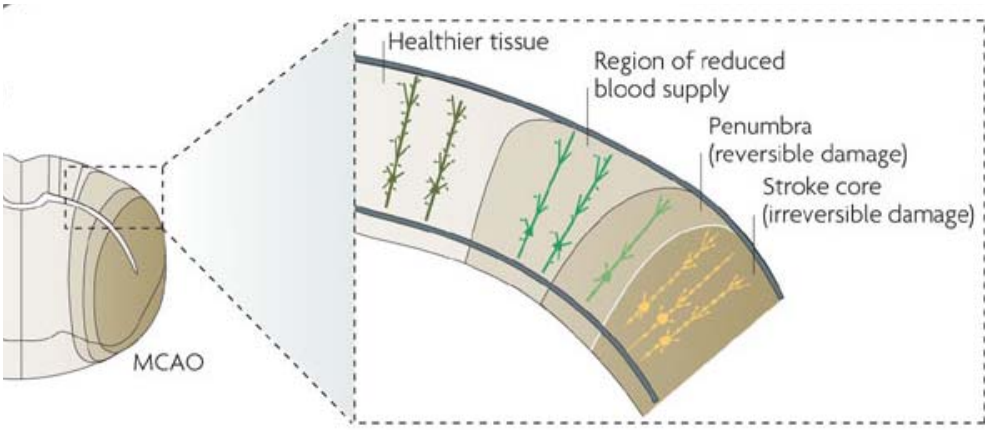

Figure 5.1 Tissue status in cortex with a gradient of blood flow (Murphy and Corbett, 2009).

Histological analysis showed that the infarct growth was a time-dependent process, and delayed ischemia developed throughout the acute and subacute phase (Figure 4.1a). It followed a progression from early infarction in the striatum to delayed infarction in the dorsolateral cortex. The striatum infarction was nearly completed or grew slowly after 24h, but the cortical infarction continued to expand until 72h (Figure 4.1a). The infarction growth process was generally consistent with other findings using the same MCAo model, despite the shorter occlusion time and different brain slices selected (Xu et al., 2006). Xu et al. analyzed the infarct development in the anterior commissure after 60 min MCAo. They found the total infarction peaked at 72h and did not change from 72h to 168h. Factors like

inflammation, edema, and apoptosis might contribute to delayed ischemia lasting for days (Figure 5.2).

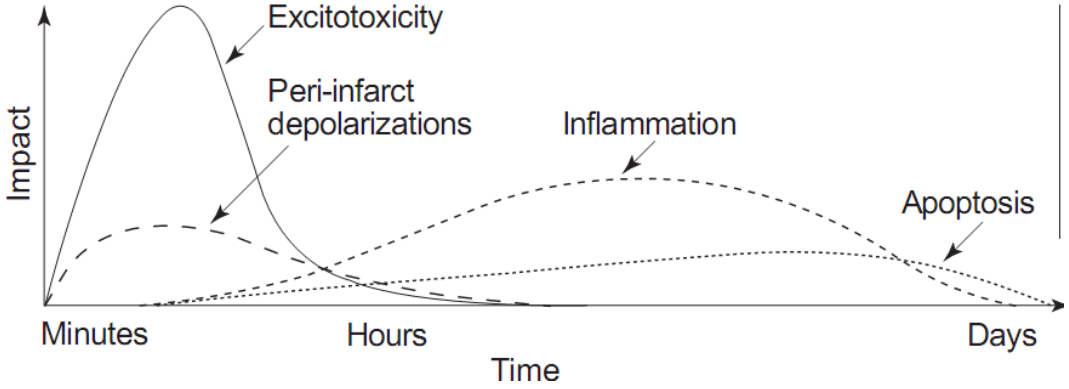

Figure 5.2 Ischemic cascades after stroke. Soon after the onset of ischemia, excitotoxicity can lethally damage neurons. In addition, excitotoxicity triggers a number of events that can further contribute to brain damage, including peri-infarct depolarization, inflammation and apoptosis (Dirnagl et al., 1999).

5.2 ECoG in focal cerebral ischemia

In this study, the spontaneous ECoG was impaired in the penumbra, with abnormalities such as a loss of alpha/beta activity. The ECoG/EEG morphology and frequency might correlate with a decreased CBF and severity of ischemia (Table 5.1). In the penumbra CBF is reduced to 12-22 ml/100g/min (Heiss, 2011).

Table 5.1 ECoG/EEG correlating with CBF reductions and degree of neural injury (Jordan, 2004)

CBF level (ml/ (100g*min))	ECoG/EEG change
35-70	Normal
25-35	Loss of fast beta frequencies
18-25	Slowing to 5-7Hz theta
12-18	Slowing to 1-4Hz delta

5.2.1 Delta and theta activities

The results showed that neural activities were significantly slowed after MCAo in the form of polymorphic delta activity (PDA) (Section 2.6.2, Section 4.3.2). PDA was generated by the interruptions of the afferent inputs from the white matter, thalamus,

or hypothalamus into the cortex. Gloor and Schaul investigated the location of structural lesions that produced localized, lateralized, or generalized slow activity in the EEG in a series of experiments and found purely cortical gray matter lesions seldom produced PDA (gray matter lesions only accounted for 7% of all cases) (Gloor et al., 1977; Schaul, 1998). Continuous delta abnormalities were associated with large white matter lesions (white matter lesions account for 93% of all cases), midline shift (a shift of the brain past its center line), and altered state of consciousness (Schaul et al., 1986). It has been reported that PDA lasting longer than 30 minutes during carotid surgery was associated with infarction and postoperative deficits. In the absence of PDA, long occlusion periods of 40 to 50 minutes were well tolerated by patients during surgery (Collice et al., 1986). In this study, PDA was persistent during the acute phase, which indicated irreversible ischemia in the striatum. The attenuation of PDA indicated that the striatum infarction was completed in the subacute phase. PDA is also reversible if blood perfusion is reestablished within certain time window (Jordan, 2004), suggesting there is a "window of reversible injury" between the early PDA and neuron death.

The theta peak was missing in the acute phase; instead, two peaks were observed within the delta band (Figure 4.3d). The 5 Hz peak might indicate theta wave slowing as a mild form of polymorphic delta activity (Schaul, 1998). Besides, the results showed that theta power recovered with a large variance from the subacute phase to the chronic phase. One possible explanation is that theta activity is state-dependent or activity-dependent. Moderate to high amplitude theta activity

indicates sleepiness; while low to moderate amplitude theta activity is associated with active wakefulness (Vyazovskiy and Tobler, 2005). As a result, theta activity is not reliable as a post-stroke physiological index (Finnigan et al., 2007).

5.2.2 Alpha and beta activities

A loss of alpha activities was observed in the ipsilesional hemisphere but not in the contralesional hemisphere after MCAo. The attenuation of alpha activities in the subacute phase might suggest delayed cortical damage in the penumbra. Since alpha activity is mostly generated by corticocortical connection (Faught, 1993), the delayed increase in alpha activity might suggest a restoration of corticocortical connections in the chronic phase (Figure 4.6a).

The alpha peak power histogram showed the time course of alpha variability from the acute phase to the chronic phase (Figure 4.8). The gradual decrease in alpha variability from the acute phase to the subacute phase might result from the mild reduction of CBF in the MCA-supplied brain regions even after reperfusion (i.e. the thalamus), which in turn altered thalamic firing patterns and perhaps decreased the variability of the thalamic firing which in turn leads to less alpha variability. Persistently poor alpha variability might be a predictor of a poor neurologic outcome (Vespa et al., 1997). In this study, the alpha variability was restored to the pre-stroke level in the chronic phase, suggesting that neural dysfunction in the penumbra was reversible.

In contrast to the full recovery of alpha activities, this study only found the partial

recovery of beta activities in the penumbra (Figure 4.6b). It is possible that the recovery of each frequency band varies by location. For example, in the temporal cortex (the infarct core), alpha power never fully recovered and remained at approximately 60% of the pre-stroke level, while beta power recovered to approximately 90% of baseline in some cortical regions (Lu et al., 2001). Therefore, the alpha activity is more closely related to functional recovery than beta activity recorded in the ischemic penumbra.

In contrast to the pattern of contralesional alpha activity, beta activity was elevated in the contralesional hemisphere than the ipsilesional hemisphere over time. This remote alternation of beta activities might reflect contralesional changes in CBF and other metabolic factors in response to an ipsilesional stroke (Andrews, 1991; Lu et al., 2001; Machado et al., 2004). Reperfusion promoted a delayed increase in the ECoG amplitude in the contralesional frontal and temporal regions (Lu et al., 2001), which might account for the elevated beta activity in the contralesional hemisphere. This contralesional response in beta activity might represent a compensatory mechanism through remote excitability or inhibition (Andrews, 1991).

5.3 Quantitative ECoG and functional recovery

In this study, sensorimotor recovery started as early as 24h, regardless of infarct growth until 72h. This observation indicated that the ischemic damage and functional recovery were two processes existing simultaneously. In the acute phase, the functional impairment might reflect damage in the ischemic core and the penumbra.

When the infarct core stopped expanding in the subacute phase, brain function could gradually recover within the penumbra (Dirnagl et al., 1999). Neuroprotective drugs that reduce infarct volume might actually inhibit functional recovery (Clarkson et al., 2010).

In this study, the intraluminal suture MCAo produced a large infarct in the cortex and striatum. Functional recovery in this model manifested the characteristics of a medium stroke and a large stroke, as described in Figure 5.3. If the lesion is localized, the adjacent cortex is involved in the functional recovery, whereas the contralesional hemisphere has to take over some functions if the lesion is large. This study showed that penumbral neural activities were highly correlated with sensorimotor recovery from the subacute phase to the chronic phase (Figure 4.10), possibly suggesting the important role of functional reorganization in the sensorimotor cortex, which was adjacent to the infarct core (barrel cortex and secondary sensory cortex). This study also noted contralesional changes in beta activity, indicating the possible role of contralesional response in promoting functional recovery after a stroke (Figure 4.6b). The results showed ipsilesional ADRs was more closely related to sensorimotor recovery than contralesional ADRs, since the contralesional alpha remained unchanged (Figure 4.6a). As a result, the recovery of ipsilesional neural activities could better predict functional recovery than contralesional neural activities in this MCAo model, since ipsilesional reorganization was reported to be more important than contralesional reorganization (Murphy and Corbett, 2009). These findings are generally in accordance with previous fMRI studies, which demonstrated that

significant contralesional sensorimotor activation occurred from 24h to 72h, and a shift from contralesional activation to ipsilesional activation was accompanied by significant improvement in neurological scores by day 14 (Dijkhuizen et al., 2003). However, the De Ryck's scores on Day 14 (7.6±1.3) were not significant different from the scores on Day 7 (7.5±1.7) in this study. It is possible that 120-min MCAo with silicon-coated suture in Dijkhuizen's study was likely to produce a larger infarct than the infarct produced in this study by the suture without a coating (Shimamura et al., 2006). As a result, the recovery of ipsilesional activation was delayed because the contralesional activation might account for functional recovery over a longer period.

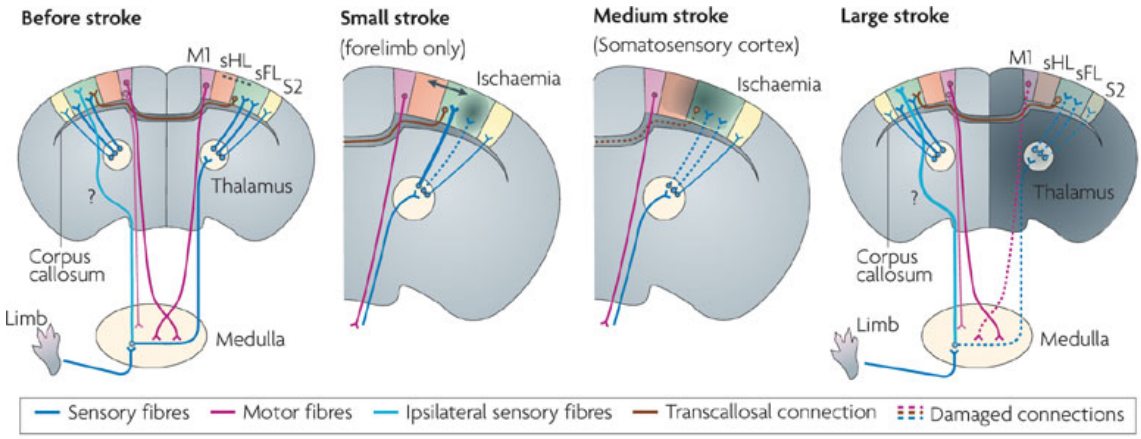

Figure 5.3 Possible mechanisms of small, medium, and large stroke recovery. For small strokes, if S1HL remains intact, it would undergo remapping and take over the function of the damaged S1FL. For medium-sized stroke, remapping might take place in the adjacent secondary sensory cortex (S2) or in M1. For large strokes, an ipsilesional pathway to the homotopic contralesional cortex is established (Murphy and Corbett, 2009).

In addition, our results showed a high correlation between ADRs and De Ryck's scores, suggesting that qEEG could be used to monitor the time course of functional recovery in addition to its usage in long-term prognostication. Good sensorimotor

functional recovery was indicated by an absence of delta activity along with preservation of background activity (alpha/beta), or by intermittent delta/theta activity with slightly asymmetrical background activity. Similar results were observed in aphasic patients (Hensel et al., 2004; Spironelli and Angrilli, 2009). It has been suggested that the preservation of fast background activity, like alpha and beta, is indicative of neural survival and a good prognosis following a stroke (Finnigan et al., 2007; Leon-Carrion et al., 2009).

Finally, ECoG changed within minutes after MCAo, but stroke rats did not exhibit sensorimotor or neurological deficits until 6h after ischemia, and it might take longer time to observe these deficits. ECoG/EEG was shown to change prior to any significant changes in clinical stroke symptoms (Finnigan et al., 2006). However, functional tests might be useful in the subacute and chronic phases, but it was difficult to conduct functional tests for comatose subjects.

5.4 Sensitivity of functional tests

The De Ryck's and beam walking tests provided information on functional recovery from different aspects. The average beam walking score was 4.9±1.5 at 168h (80% of pre-stroke beam walking score); whereas the average De Ryck's score was 7.6± 1.3 (50% of pre-stroke De Ryck's score) and all the rats could not fully restore their sensorimotor function even after 14 days. One possible explanation is that the hindlimb cortex is the outer boundary of the penumbra, and its dysfunction might be reversible; whereas the forelimb cortex is the inner bounder of penumbra and it

might lose its function permanently (Table 2.1). These findings suggested that the spontaneous recovery could occur more quickly in some tasks (e.g. beam walking) than in other tasks (e.g. De Ryck' test) (Hunter et al., 2000).

The sensitivity of a functional test relates to the specific brain regions involved in the task (Brooks and Dunnett, 2009), depending on the correspondence between the specific motor control provided by the affected system (Lalonde and Strazielle, 2007). This study chose the sensorimotor cortex as the targeted brain region which was sensitive to the effects of MCAo, thereby allowing us to evaluate the relationship between changes in neural response and behavioral parameters (Virley et al., 2000).

5.5 Clinical relevance

EEG recording is able to reveal post-stroke neurophysiological processes in the brain. Polygraphic EEG, spectral analyses, and qEEG are complementary in detecting the different features of EEG abnormalities (Section 4.3, Section 4.4 and Section 4.5). For example, seizures and PLED are best observed by visually inspecting of the polygraph EEG, while detailed EEG power distribution could be obtained by spectral analysis. As the results suggested, ECoG changed before functional deficits were evident (Section 5.3), thus it is postulated continuous EEG can provide information prior to clinical symptom onset after acute ischemic stroke.

The ADRs remained below 50% of the pre-stroke level from 24h to 48h, which is a sensitive indicator for delayed ischemia from 48h to 72h. The ADRs reached 50% of the pre-stroke level at 72h, and the infarct did not subsequently expand. This finding

suggests that qEEG is useful for localizing acute brain malfunctions before cerebral lesions mature. qEEG parameters, such as ADRs and alpha/beta peak power variability, can distinguish between reversible and irreversible ischemic damage, while MRI parameters (i.e. ADC) do not necessarily indicate irreversible tissue damage (Jordan, 2004).

5.6 Suggestions for future studies

1. This study determined the successful induction of ischemia by observing ECoG amplitude reduction and polymorphic delta activity in ischemic penumbra. Future studies could use laser Doppler flowmetry to study coupling between blood flow reduction and ECoG when inducing ischemia.
2. This study measured neural activity with two electrodes placed on the bilateral sensorimotor cortex (one electrode for each hemisphere). A multi-channel electrode array covering the infarct core (i.e., barrel cortex), penumbra (S1HL, S1FL), and normal tissue (M1, M2) could be used in future ECoG studies. These areas may have different degrees of injury/recovery, and it is likely that the neuronal activities in these three areas are different. The advantage of multi-channel ECoG array is to study the neuronal response in these areas separately, and to link ECoG activities with parameters specific to hindlimb/forelimb sensorimotor function.
3. In clinical situations, EEG can provide a rapid, bedside assessment of post-stroke brain functions. In conjunction with MRI, EEG with low-density electrodes

placed around the penumbra can be used in the future study to identify background activity (e.g. alpha/beta activity), evoked field potentials, and spike bursts in stroke patients.

CHAPTER 6 CONCLUSIONS

This study demonstrated the feasibility of an ECoG monitoring system in a rat model of focal cerebral ischemia, and investigated the effects of unilateral stroke on bilateral ECoG as well as the correlation between quantitative ECoG parameters in penumbra (ADR, peak power variability) and functional recovery from the acute phase to the chronic phase after stroke.

Ischemic ECoG reflected the temporal course of infarct development in MCAo model. Polymorphic delta activity was associated with striatum infarction in the acute phase, whereas a prolonged suppression in alpha and beta activities might be associated with delayed cortical infarction in the subacute phase, which was also confirmed by TTC staining in histological analysis. Alpha activities were restored to the pre-stroke level while the beta activities did not fully recover in the penumbra even after the chronic phase (168 hours). Improvement in ADRs was highly correlated with sensorimotor functional recovery from 24 hours to 168 hours. Decreased alpha/beta variability in the subacute phase might indicate reversible dysfunction in the penumbra. These findings provided information on the potential application of ECoG in focal cerebral ischemia for quantitative studies of brain acitivies after stroke.

APPENDIX

Form 2

Licence to Conduct Experiments

Name : ZHANG Shaojie [Ref No.: (09-67) in DH/HA&P/8/2/4 Pt.2]

Address : Department of Health Technology and Informatics, The Hong Kong Polytechnic University

By virtue of section 7 of the Animals (Control of Experiments) Ordinance, Chapter 340, the above-named is hereby licensed to conduct the type of experiment(s), at the place(s) and upon the conditions, hereinafter mentioned.

Type of experiment(s)

Rats will be used in the experiment. Under general anaesthesia, neuromuscular stimulation electrodes will be implanted at the hindlimbs and the cortex of the animals. On Day 13 of the experiment, stroke will be induced by middle cerebral artery occlusion under general anaesthesia. Analgesic will be given after the operations. Neuromuscular electrical stimulation (NMES) on hindlimb muscles and functional assessments will be conducted before and after stroke. Throughout the experiment, conditions of the animals will be monitored. Animals that show signs of distress will be sacrificed with an overdose of anaesthetic. At the end of the experiment, the animals will be sacrificed with an overdose of anaesthetic. Brain tissues will then be harvested for analysis.

Place(s) where experiment(s) may be conducted

Centralised Animal Facilities, Room 1426, 14/F, Y Core, The Hong Kong Polytechnic University

Conditions

1. Such experiment(s) may only be conducted for the following purposes-

   (a) To investigate the effects of NMES after stroke using animal models;
   (b) To find NMES training schemes that can maximize motor functional recovery and minimize the loss in brain tissue.

2. This licence is valid from 1 September 2009 to 31 August 2011

Dated 1 September 2009

DEPARTMENT OF HEALTH 衞生署 HONG KONG

Licensing Authority

REFERENCES

Abraham H, Somogyvari A, Maderdrut JL, Vigh S, Arimura A. Filament size influences temperature changes and brain damage following middle cerebral artery occlusion in rats. Experimental Brain Research 2002; 142: 131–138.

Andrews RJ. Transhemispheric diaschisis. A review and comment. Stroke 1991; 22: 943–949.

Bederson J, Pitts L, Tsuji M, Nishimura M, Davis R, Bartkowski H. Rat middle cerebral artery occlusion: evaluation of the model and development of a neurologic examination. Stroke 1986; 17: 472–476.

Bouët V, Freret T, Toutain J, Divoux D, Boulouard M, Schumann-Bard P. Sensorimotor and cognitive deficits after transient middle cerebral artery occlusion in the mouse. Experimental Neurology 2007; 203: 555–567.

Brooks SP, Dunnett SB. Tests to assess motor phenotype in mice: a user's guide. Nature reviews. Neuroscience 2009; 10: 519–29.

Busch E, Krüger K, Hossmann KA. Improved model of thromboembolic stroke and rt-PA induced reperfusion in the rat. Brain Research 1997; 778: 16–24.

Carmichael ST. Rodent models of focal stroke: size, mechanism, and purpose. NeuroRx 2005; 2: 396–409.

Chiganos TC, Jensen W, Rousche PJ. Electrophysiological response dynamics during focal cortical infarction. Journal of neural engineering 2006; 3: L15–22.

Claassen J, Hirsch LJ, Kreiter KT, Du EY, Connolly ES, Emerson RG, Mayer SA. Quantitative continuous EEG for detecting delayed cerebral ischemia in patients with poor-grade subarachnoid hemorrhage. Clinical neurophysiology 2004; 115: 2699–710.

Clarke KA, Still J. Development and consistency of gait in the mouse. Physiology & Behavior 2001; 73: 159–164.

Clarkson AN, Huang BS, Macisaac SE, Mody I, Carmichael ST. Reducing excessive GABA-mediated tonic inhibition promotes functional recovery after stroke. Nature 2010; 468: 305–9.

Collice M, Arena O, Fontana RA, Mola M, Galbiati N. Role of EEG monitoring and cross-clamping duration in carotid endarterectomy. Journal of Neurosurgery 1986; 65: 815–819.

Daly JJ, Wolpaw JR. Brain computer interfaces in neurological rehabilitation. Lancet Neurology 2008; 7: 1032–1043.

Dijkhuizen RM, Singhal AB, Mandeville JB, Wu O, Halpern EF, Finklestein SP, Rosen BR, Lo EH. Correlation between brain reorganization, ischemic damage and neurologic status after transient focal cerebral ischemia in rats: a functional

magnetic resonance imaging study. The Journal of neuroscience 2003; 23: 510–7.

Dirnagl U, Iadecola C, Moskowitz MA. Pathobiology of ischaemic stroke: an integrated view. Trends in neurosciences 1999; 22: 391–7.

Dogan A, Bakaya MK, Rao VL, Rao AM, Dempsey RJ. Spontaneous hyperthermia and its mechanism in the intraluminal suture middle cerebral artery occlusion model of rats. Neurological Research 1999; 20: 265–270.

Doyle KP, Simon RP, Stenzel-Poore MP. Mechanisms of ischemic brain damage. Neuropharmacology 2008; 55: 310–8.

Dunham NW, Miya TS. A note on a simple apparatus for detecting neurological deficit in rats and mice. Journal of the American Pharmaceutical Association 1957; 46: 208–209.

Durukan A, Tatlisumak T. Acute ischemic stroke: overview of major experimental rodent models, pathophysiology, and therapy of focal cerebral ischemia. Pharmacology, biochemistry, and behavior 2007; 87: 179–97.

Elsaesser-Schmid R, Zausinger S, Hungerhuber E, Baethmann A, Reulen HJ, Garcia JH. A critical ceevaluation of the intraluminal thread model of focal cerebral ischemia: evidence of inadvertent premature reperfusion and subarachnoid hemorrhage in rats by laser-Doppler flowmetry. Stroke 1998; 29: 2162–2170.

Emerich DF, Dean RL, Bartus RT. The role of leukocytes following cerebral ischemia: pathogenic variable or bystander reaction to emerging infarct? Experimental Neurology 2002; 173: 168–181.

Fabricius M, Fuhr S, Bhatia R, Boutelle M, Hashemi P, Strong AJ, Lauritzen M. Cortical spreading depression and peri-infarct depolarization in acutely injured human cerebral cortex. Brain 2006; 129: 778–90.

Faught E. Current role of electroencephalography in cerebral ischemia. Stroke 1993; 24: 609–613.

Feeney DM, Gonzalez A, Law WA. Amphetamine, haloperidol, and experience interact to affect rate of recovery after motor cortex injury. Science 1982; 217: 855–857.

Finnigan SP, Rose SE, Chalk JB. Rapid EEG changes indicate reperfusion after tissue plasminogen activator injection in acute ischaemic stroke. Clinical neurophysiology 2006; 117: 2338–9.

Finnigan SP, Rose SE, Walsh M, Griffin M, Janke AL, McMahon KL, Gillies R, Strudwick MW, Pettigrew CM, Semple J, Brown J, Brown P, Chalk JB. Correlation of quantitative EEG in acute ischemic stroke with 30-day NIHSS score: comparison with diffusion and perfusion MRI. Stroke 2004; 35: 899–903.

Finnigan SP, Walsh M, Rose SE, Chalk JB. Quantitative EEG indices of sub-acute ischaemic stroke correlate with clinical outcomes. Clinical neurophysiology 2007; 118: 2525–32.

Friedman D, Claassen J. Quantitative EEG and cerebral ischemia. Clinical Neurophysiology 2010; 121: 1707–8.

Fujioka H, Kaneko H, Suzuki SS, Mabuchi K. Hyperexcitability-associated rapid plasticity after a focal cerebral ischemia. Stroke 2004; 35: e346–8.

Furlan M, Marchal G, Viader F, Derlon JM, Baron JC. Spontaneous neurological recovery after stroke and the fate of the ischemic penumbra. Annals of neurology 1996; 40: 216–26.

Fuxe K, Bjelke B, Andbjer B, Grahn H, Rimondini R, Agnati LF. Endothelin-1 induced lesions of the frontoparietal cortex of the rat. A possible model of focal cortical ischemia. NeuroReport 1997; 8: 2623–2629.

Gloor P, Ball G, Schaul N. Brain lesions that produce delta waves in the EEG. Neurology 1977; 27: 326–333.

Goldlust EJ, Paczynski RP, He YY, Hsu CY, Goldberg MP. Automated measurement of infarct size with scanned images of triphenyltetrazolium chloride-stained rat brains. Stroke 1996; 27: 1657–1662.

Harri M, Lindblom J, Malinen H, Hyttinen M, Lapveteläinen T, Eskola S, Helminen HJ. Effect of access to a running wheel on behavior of C57BL/6J mice. Laboratory Animal Science 1999; 49: 401–405.

Hartings JA, Rolli ML, Lu XC, Tortella FC. Delayed secondary phase of peri-infarct depolarizations after focal cerebral ischemia: relation to infarct growth and neuroprotection. The Journal of neuroscience 2003; 23: 11602–10.

Hartings JA, Tortella FC, Rolli ML. AC electrocorticographic correlates of peri-infarct depolarizations during transient focal ischemia and reperfusion. Journal of cerebral blood flow and metabolism 2006; 26: 696–707.

Hartings JA, Williams AJ, Tortella FC. Occurrence of nonconvulsive seizures, periodic epileptiform discharges, and intermittent rhythmic delta activity in rat focal ischemia. Experimental Neurology 2003; 179: 139 –149.

He Z, Yamawaki T, Yang S, Day AL, Simpkins JW, Naritomi H, Rosenblum WI. Experimental model of small deep infarcts involving the hypothalamus in rats : changes in body temperature and postural reflex. Stroke 1999; 30: 2743–2751.

Heiss WD. The ischemic penumbra: correlates in imaging and implications for treatment of ischemic stroke. Cerebrovascular diseases 2011; 32: 307–320.

Hensel S, Rockstroh B, Berg P, Elbert T, Schönle PW. Left-hemispheric abnormal EEG activity in relation to impairment and recovery in aphasic patients. Psychophysiology 2004; 41: 394–400.

Hermann DM, Kilic E, Hata R, Hossmann KA, Mies G. Relationship between metabolic dysfunctions, gene responses and delayed cell death after mild focal cerebral ischemia in mice. Neuroscience 2001; 104: 947–55.

Hofmeijer J, van Putten M. Ischemic cerebral damage: an appraisal of synaptic failure. Stroke 2012; 43: 607–15.

Hossmann KA. Cerebral ischemia: models, methods and outcomes. Neuropharmacology 2008; 55: 257–70.

Hunter AJ, Hatcher J, Virley D, Nelson P, Irving E, Hadingham SJ, Parsons AA. Functional assessments in mice and rats after focal stroke. Neuropharmacology 2000; 39: 806–16.

Johnston SC, Rothwell PM, Nguyen-Huynh MN, Giles MF, Elkins JS, Bernstein AL, Sidney S. Validation and refinement of scores to predict very early stroke risk after transient ischaemic attack. Lancet 2007; 369: 283–92.

Jolkkonen J, Puurunen K, Rantakomi S, Harkonen A, Haapalinna A, Sivenius J. Behavioral effects of the alpha(2)-adrenoceptor antagonist, atipamezole, after

focal cerebral ischemia in rats. European journal of pharmacology 2000; 400: 211–9.

Jordan KG. Emergency EEG and continuous EEG monitoring in acute ischemic stroke. Journal of clinical neurophysiology 2004; 21: 341–52.

Ke Z, Yip SP, Li L, Zheng XX, Tong KY. The effects of voluntary, involuntary, and forced exercises on brain-derived neurotrophic factor and motor function recovery: a rat brain ischemia model. PloS one 2011; 6: e16643.

Kelly KM, Jukkola PI, Kharlamov EA, Downey KL, McBride JW, Strong R, Aronowski J. Long-term video-EEG recordings following transient unilateral middle cerebral and common carotid artery occlusion in Long-Evans rats. Experimental neurology 2006; 201: 495–506.

Kloss CU, Thomassen N, Fesl G, Martens KH, Yousri TA, Hamann GF. Tissue-saving infarct volumetry using histochemistry validated by MRI in rat focal ischemia. Neurological Research 2002; 24: 713–718.

Koizumi J, Yoshida Y, Nakazawa T, Ooneda G. Experimental studies of ischemic brain edema: a new experimental model of cerebral embolism in rats in which recirculation can be introduced in the ischemic area. Japan Journal of Stroke 1986; 8: 1–8.

Lalonde R, Strazielle C. Brain regions and genes affecting postural control. Progress in neurobiology 2007; 81: 45–60.

Leon-Carrion J, Martin-Rodriguez JF, Damas-Lopez J, Dominguez-Morales MR. Delta-alpha ratio correlates with level of recovery after neurorehabilitation in patients with acquired brain injury. Brain Injury 2009; 120: 1039–1045.

Leung TW, Lau AYL, Graham CA, Wong EHC, Soo YOY, Wong LKS. Thrombolysis for acute ischaemic stroke is evidence-based. Hong Kong medical journal 2011; 17: 168.

Leuthardt EC, Schalk G, Moran D, Ojemann JG. The emerging world of motor neuroprosthetics: a neurosurgical perspective. Neurosurgery 2006; 59: 1–14.

Leuthardt EC, Schalk G, Roland J, Rouse A, Moran DW. Evolution of brain-computer interfaces: going beyond classic motor physiology. Neurosurgical focus 2009; 27: E4.

Li Y, Powers C, Jiang N, Chopp M. Intact, injured, necrotic and apoptotic cells after focal cerebral ischemia in the rat. Journal of the neurological sciences 1998; 156: 119–32.

Liu F, Schafer DP, McCullough LD. TTC, fluoro-Jade B and NeuN staining confirm evolving phases of infarction induced by middle cerebral artery occlusion. Journal of neuroscience methods 2009; 179: 1–8.

Longa E, Weinstein P, Calson S, Cummins R. Reversible middle cerebral artery occlusion without craniectomy in rats. Stroke 1989; 20: 84–91.

Lu XC, Williams AJ, Tortella FC. Quantitative electroencephalography spectral analysis and topographic mapping in a rat model of middle cerebral artery occlusion. Neuropathology and applied neurobiology 2001; 27: 481–95.

Lu XC, Williams AJ, Wagstaff JD, Tortella FC, Hartings JA. Effects of delayed intrathecal infusion of an NMDA receptor antagonist on ischemic injury and peri-infarct depolarizations. Brain research 2005; 1056: 200–8.

Ma J, Zhao L, Nowak TS. Selective, reversible occlusion of the middle cerebral artery in rats by an intraluminal approach. Optimized filament design and methodology. Journal of Neuroscience Methods 2006; 156: 76–83.

Machado C, Cuspineda E, Valdés P, Virues T, Llopis F, Bosch J, Aubert E, Hernández E, Pando A, Alvarez MA, Barroso E, Galán L, Avila Y. Assessing acute middle cerebral artery ischemic stroke by quantitative electric tomography. Clinical EEG and neuroscience 2004; 35: 116–24.

Macrae IM, Robinson MJ, Graham DI, Reid JL, McCulloch J. Endothelin-1-induced reductions in cerebral blood flow: dose dependency, time course, and neuropathological consequences. Journal of cerebral blood flow and metabolism 1993; 13: 276–284.

Maltez J, Hyllienmark L, Nikulin VV, Brismar T. Time course and variability of power in different frequency bands of EEG during resting conditions. Neurophysiologie clinique 2004; 34: 195–202.

Metz GA, Antonow-Schlorke I, Witte OW. Motor improvements after focal cortical ischemia in adult rats are mediated by compensatory mechanisms. Behavioural Brain Research 2005; 162: 71–82.

Miche VP, Dénes T. Continuous quantitative EEG monitoring in hemispheric stroke patients using the brain symmetry index. Stroke 2004; 35: 2489–2492.

Mies G, Lijima T, Hossmann KA. Correlation between peri-infarct DC shifts and ischemic neuronal damage in rat. NeuroReport 1993; 4: 709–711.

Murphy TH, Corbett D. Plasticity during stroke recovery: from synapse to behaviour. Nature Reviews Neuroscience 2009; 10: 861–72.

Murri L, Gori S, Massetani R, Bonanni E, Marcella F, Milani S. Evaluation of acute ischemic stroke using quantitative EEG: a comparison with conventional EEG and CT scan. Neurophysiologie Clinique 1998; 28: 249–257.

Park HJ, Jeong DU, Park KS. Automated detection and elimination of periodic ECG artifacts in EEG using the energy interval histogram method, IEEE Transactions on Biomedical Engineering 2002;

Paxinos G, Watson C. The rat brain in stereotaxic coordinates, 6th ed 2007; Academic Press.

Popp A, Jaenisch N, Witte OW, Frahm C. Identification of Ischemic Regions in a Rat Model of Stroke. PLoS ONE 2009; 4: 8.

Roger VL, Go AS, Lloyd-Jones DM, Adams RJ, Berry JD, Brown TM, Carnethon MR, Dai S, de Simone G, Ford ES, Fox CS, Fullerton HJ, Gillespie C, Greenlund KJ, Hailpern SM, Heit J a, Ho PM, Howard VJ, Kissela BM, Kittner SJ, Lackland DT, Lichtman JH, Lisabeth LD, Makuc DM, Marcus GM, Marelli A, Matchar DB, McDermott MM, Meigs JB, Moy CS, Mozaffarian D, Mussolino ME, Nichol G, Paynter NP, Rosamond WD, Sorlie PD, Stafford RS, Turan TN, Turner MB, Wong ND, Wylie-Rosett J. Heart disease and stroke statistics 2011 update: a report from the American Heart Association. Circulation 2011; 123: e18–e209.

De Ryck M, Van Reempts J, Borgers M, Wauquier A, Janssen PA. Photochemical stroke model: flunarizine prevents sensorimotor deficits after neocortical infarcts in rats. Stroke 1989; 20: 1383–90.

Schallert T, Fleming SM, Leasure JL, Tillerson JL, Bland ST. CNS plasticity and assessment of forelimb sensorimotor outcome in unilateral rat models of stroke, cortical ablation, parkinsonism and spinal cord injury. Neuropharmacology 2000; 39: 777–787.

Schaul N. The fundamental neural mechanisms of electroencephalography. Electroencephalography and clinical neurophysiology 1998; 106: 101–7.

Schaul N, Green L, Peyster R, Gotman J. Structural determinants of electroencephalographic findings in acute hemispheric lesions. Annals of Neurology 1986; 20: 703–711.

Sharbrough FW, Messick JM, Sundt TM. Cerebral blood flow measurements and electroencephalograms during carotid endarterectomy. Stroke 1973; 4: 674–683.

Shimamura N, Matchett G, Tsubokawa T, Ohkuma H, Zhang J. Comparison of silicon-coated nylon suture to plain nylon suture in the rat middle cerebral artery occlusion model. Journal of Neuroscience Methods 2006; 156: 161–165.

Sicard KM, Henninger N, Fisher M, Duong TQ, Ferris CF. Differential recovery of multimodal MRI and behavior after transient focal cerebral ischemia in rats. Journal of cerebral blood flow and metabolism 2006; 26: 1451–62.

Sigler A, Mohajerani MH, Murphy TH. Imaging rapid redistribution of sensory-evoked depolarization through existing cortical pathways after targeted stroke in mice. Proceedings of the National Academy of Sciences 2009; 106: 11759–64.

Soltanian-Zadeh H, Pasnoor M, Hammoud R, Jacobs MA, Patel SC, Mitsias PD, Knight RA, Zheng ZG, Lu M, Chopp M. MRI tissue characterization of

experimental cerebral ischemia in rat. Journal of magnetic resonance imaging 2003; 17: 398–409.

Sommer C. Histology and infarct volume determination, in: Dirnagl, U. (Ed.), Rodent Models of Stroke 2010; Humana Press, Totowa, NJ, pp. 213–226.

Spironelli C, Angrilli A. EEG delta band as a marker of brain damage in aphasic patients after recovery of language. Neuropsychologia 2009; 47: 988–994.

Thakor NV, Tong S. Advances in quantitative electroencephalogram analysis methods. Annual review of biomedical engineering 2004; 6: 453–95.

Tortella FC, Britton P, Williams A, Lu XC, Newman AH. Neuroprotection (focal ischemia) and neurotoxicity (electroencephalographic) studies in rats with AHN649, a 3-amino analog of dextromethorphan and low-affinity N-methyl-D-aspartate antagonist. The Journal of pharmacology and experimental therapeutics 1999; 291: 399–408.

Ungerstedt U, Arbuthnott GW. Quantitative recording of rotational behvior in rats after 6-hydroxydopamine lesions of the nigrostriatal dopamine system. Synapse 1970; 24: 485–493.

Vespa PM, Nuwer MR, Juhasz C, Alexander M, Nenov V, Martin N, Becker DP. Early detection of vasospasm after acute subarachnoid hemorrhage using

continuous EEG ICU monitoring. Electroencephalography and clinical neurophysiology 1997; 103: 607–15.

Virley D, Beech JS, Smart SC, Williams SC, Hodges H, Hunter AJ. A temporal MRI assessment of neuropathology after transient middle cerebral artery occlusion in the rat: correlations with behavior. Journal of cerebral blood flow and metabolism 2000; 20: 563–82.

Vyazovskiy VV, Tobler I. Theta activity in the waking EEG is a marker of sleep propensity in the rat. Brain Research 2005; 1050: 64–71.

Watson BD, Dietrich WD, Busto R, Wachtel MS, Ginsberg MD. Induction of reproducible brain infarction by photochemically initiated thrombosis. Annals of Neurology 1985; 17: 497–504.

Whishaw IQ, O'Connor WT, Dunnett SB. The contributions of motor cortex, nigrostriatal dopamine and caudate putamen to skilled forelimb use in the rat. Brain 1986; 109: 805–843.

Williams AJ, Lu XC, Hartings JA, Tortella FC. Neuroprotection assessment by topographic electroencephalographic analysis: effects of a sodium channel blocker to reduce polymorphic delta activity following ischaemic brain injury in rats. Fundamental & clinical pharmacology 2003; 17: 581–93.

Xu X, Zhang S, Yan W, Li X, Zhang H, Zheng X. Development of cerebral infarction, apoptotic cell death and expression of X-chromosome-linked inhibitor of apoptosis protein following focal cerebral ischemia in rats. Life sciences 2006; 78: 704–12.

Zhang S, Boyd J, Delaney K, Murphy TH. Rapid reversible changes in dendritic spine structure in vivo gated by the degree of ischemia. The Journal of neuroscience : the official journal of the Society for Neuroscience 2005; 25: 5333–8.

Zhang X, Zhang RL, Zhang ZG, Chopp M. Measurement of neuronal activity of individual neurons after stroke in the rat using a microwire electrode array. Journal of neuroscience methods 2007; 162: 91–100.